Journal of South American Earth Sciences 100 (2020) 102558

Contents lists available at ScienceDirect

Journal of South American Earth Sciences

journal homepage: www.elsevier.com/locate/jsames

The geodynamic history of the Famatinian arc, Argentina: A record of exposed geology over the type section (latitudes 27°- 33° south)

Juan E. Otamendi[a,*], Eber A. Cristofolini[a], Augusto Morosini[b], Paula Armas[a], Alina M. Tibaldi[a], Giuliano C. Camilletti[a]

[a] CONICET, Departamento de Geología, Universidad Nacional de Río Cuarto, Campus Universitario, X5804BYA, Río Cuarto, Argentina
[b] CONICET, Departamento de Geología, Universidad Nacional de San Luis, D5700HHW, San Luis, Argentina

ARTICLE INFO

Keywords:
Famatinian arc
Arc crust
Collision orogeny
Gondwana margin
Geodynamics

ABSTRACT

The Famatinian arc, over central-western Argentina, is one of the few examples of exposed crustal arc cross-section in the world. This Paleozoic magmatic arc and orogenic system on the Earth's surface offers unique insights into the nature of whole-arc processes, continental crust generation, and preservation. A detailed account of birth, growth, and closure is integrated throughout the region, and the entire geodynamic history of the Famatinian arc is presented. The Famatinian magmatic arc grew during a single-cycle episode that spanned a few tens of million years. Upon waning of the Cambrian Pampean orogen, an Upper Cambrian – Lower Ordovician marginal and open sea basin developed mostly on the recently stabilized Cambrian crystalline crust and was flooded by a turbidite wedge. Typical subduction zone magmatism resumed outboard of the Pampean orogen in the Lower Ordovician. After about 20 My of magmatism driven by subduction zone dynamics at plate scale, magmatism waned and stopped with the entry of a Laurentia-rifted continental microplate in the subduction zone. A full phase of a mountain-building process accompanied the continent-arc collision. The orogenic collapse occurred during the Devonian, ending the Famatinian system after nearly 150 My of magmatic arc, plate convergence, and continent-arc collision development on the proto-Andean Gondwana margin.

1. Introduction

The past 30 years of research, or so, has seen a particular focus on the geodynamic history of the West Gondwana proto-Andean margin (Pankhurst and Rapela, 1998; Keppie and Ramos, 1999). Over this margin, the Famatinian cycle initiated the longest Paleozoic subduction system that turned into being a lasting-lived Phanerozoic destructive boundary along the length of the South American plate (Ramos, 2018; Rapela et al., 2018; Oliveros et al., 2020). Since the pioneer studies of modern era (e.g., Rapela et al., 1992; Mannheim, 1993; Mángano and Buatois, 1996; Toselli et al., 1996), hundreds of research articles focused on characterizing the nature of the Famatinian arc, and its tectonic setting, magmatic evolution, magmatic timing, and deformation history. Results obtained after three decades of modern research are integrated, discussed, and reviewed with the objective of presenting an update on the Famatinian arc, a natural example gaining interest in the geoscientific community (Paterson and Ducea, 2015; Jagoutz and Klein, 2018; Chin et al., 2018; Bachmann and Huber, 2018; Ratschbacher et al., 2019).

Our line of arguments follows the principle of uniformitarianism. The aim is at working out a model for an ancient arc under the same principles as Geoscientists use to investigate active magmatic arcs. As such, our conceptual framework is that the characteristic petrologic expression of arc magmatism is the consequence of subduction zone geodynamics (Ringwood, 1974; McCulloch and Gamble, 1991; Stern, 2002). It is, thereby, a wet upwelling flows induced by a melt/fluid component released from the subducting slab that partially melts a corner-flowing mantle wedge (Tatsumi et al., 1986; Davies and Stevenson, 1992; Schmidt and Poli, 1998). Progressively oxidized melts ascend through a canalized network, fertilize the overlaying ambient mantle wedge, and eventually cross the mantle-crust seismic boundary (Kelley and Cottrell, 2009; Tollan and Hermann, 2019). Within the overriding plate, the chemistry of subduction-related primitive magmas varies within a well-defined range and spans broadly similar in both continental and oceanic arcs (DeBari, 1997; Kelemen et al., 2003a; Schmidt and Jagoutz, 2017). These works showed that crustal density structures and their effect on intra-crustal differentiation play a role in controlling the composition and relative volumes of volcanic outputs. So, our approach is rather simplistic because the building arc process changes with arc maturation and arc-scale tectonic stress (Plank and

* Corresponding author.
E-mail address: jotamendi@exa.unrc.edu.ar (J.E. Otamendi).

https://doi.org/10.1016/j.jsames.2020.102558
Received 3 December 2019; Received in revised form 28 February 2020; Accepted 6 March 2020
Available online 14 March 2020

Langmuir, 1988; Lee et al., 2015; Cao and Paterson, 2016). Remarkably, we are learning new concepts at the same time as we better understand the Famatinian arc. Now, it becomes clear that a transcrustal magmatic column drives petrological diversity from the petrological Moho to the volcanic plumbing system (Bachmann and Bergantz, 2008; Cashman et al., 2017). Another new view is that subarc temperature conditions in continental and oceanic subduction zones are significantly higher (200–300 °C) than predicted by canonical thermal models (Jones et al., 2018). Beneath frontal arcs, a thermally eroded lithosphere leaves a petrological column rooted in the mantle wedge as dynamic mass exchange across the mantle-crust boundary sweeps arc cumulate back into the mantle (England and Katz, 2010; Lieu and Stern, 2019). As shown by Kelemen et al. (2003b), the high geothermal gradient beneath frontal arcs allowed us explaining the distribution of P-T estimates of the Famatinian arc (Tibaldi et al., 2013).

We begin observing that a feasible geological integration of the ancient Famatinian arc must explain the first-order petrological, stratigraphic, and structural features, as observed today, these are: 1) spanning from the Cambrian - Ordovician boundary to the Middle Ordovician, sedimentary, volcano-sedimentary and volcanic successions deposited within deep to shallow marine environments and around subaqueous and subaerial volcanoes, in environments where the near volcano successions laterally transgressed into reworked turbidite-like volcaniclastic deposits and distal deeper marine sediments (Mángano and Buatois, 1996; Astini, 1998; Verdecchia et al., 2007; Armas et al., 2018); 2) the entire plutonic and volcanic column was generated in a time span of about 20 My (491–467 Ma), but the great mass of the magmatic crust was produced during a *ca.* 10 My period (474–467 Ma) of the Lower - Middle Ordovician (Ducea et al., 2010, 2017; Rapela et al., 2018); 3) both the magmatic arc and the backarc are differentially exhumed along their axis, but the plutonic batholith forms a coherent magmatic column and exposed a complete crustal arc section (DeBari, 1994; Tibaldi et al., 2013); 4) over the Sierras Pampeanas segment (30° – 33° S) the bulk of the arc and backarc was shortened to end about one half of its original width (Christiansen et al., 2019), while virtually all of the fore-arc basins and trench-accretion prisms were tectonically vanished (Astini and Dávila, 2004; Otamendi et al., 2008; Cristofolini et al., 2014).

After presenting observations, we discuss each of the problems from the perspective of the data. Here we stress to integrate all of the particular and striking geological features in an evolutionary model of the Famatinian arc. We accept that an incompletely preserved geological record biases the observations and that there are natural causes to unravel using a large data set. Nevertheless, we might claim that knowledge is at a point where a geodynamic model explains the range of phenomena preserved in the ancient Famatinian arc. The article presents the observation and discussion using present-day coordinates.

2. Observations and measurements

2.1. The Famatinian arc: major stratigraphic units between 27°- 33° south

The Famatinian arc is one of the largest and best exposed to an early Paleozoic batholith which formed along the paleo-Pacific Gondwana margin. Over Argentina, it makes an almost continuous outcrop between 20° and 33° S, is underlying post-Carboniferous sedimentary basins between 33° and 40° S, and appears sporadically within north-eastern Patagonia (Fig. 1). Of key interest here is the 200-km-wide section at the latitude of the Sierra de Famatina upon which the arc is named (Toselli et al., 1996; Saavedra et al., 1998; Pankhurst et al., 1998). In a geodynamic perspective, the Famatinian arc is genetically related to east-dipping subduction represented by the backarc metamorphic belt bordering the preceding peri-Gondwanan Pampean orogen (Fig. 1). Differential exhumation exposed two major components. The largest one is a crystalline basement that consists of a Cordilleran-type batholithic belt flanked to the east by a high-grade metamorphic sequence (Toselli et al., 1996; DeBari, 1994; Pankhurst et al., 1998; Saavedra et al., 1998). The other component is a geographically dispersed but locally thick succession of sedimentary and volcano-sedimentary rocks that host volcanic sills, dikes, and lava domes (Mannheim, 1993; Mángano and Buatois, 1996; Astini, 2003).

The plutonic regional-scale Cordilleran-type batholiths of the Famatinian arc extend over the Sierras Pampeanas segment (28° to 33° S). The Famatinian batholith is divided axially into an I-type dominated plutonic belt and an S-type dominated granitic belt (Toselli et al., 1996; Pankhurst et al., 2000; Grosse et al., 2011). The predominant igneous rocks in regional-scale batholiths are calc-alkaline metaluminous I-type granitoids with subordinate peraluminous felsic granitoids within the sierras Famatina, Chepes, Las Minas-Ulapes, and Valle Fértil-La Huerta. The opposite is the case in other ranges dominated by peraluminous and felsic Famatinian plutonic rocks, among them sierras Fiambalá, Capillita and Zapata. The boundary between the western I-type and eastern S-type batholithic belts is observable in the Sierra de Velasco (Grosse et al., 2011).

The contiguous eastern metamorphic belt is mostly made up of high-T low-P metasedimentary rocks and gradually shrinks southward (Fig. 1). Similar metasedimentary rocks like those of the backarc belt occur as septa scattered within the plutonic batholith. The onset of regional low-P high-T metamorphism affecting sedimentary strata in a backarc setting is diachronic along the arc strike, it began earlier than about 505 Ma to the north of 27° S (Wolfram et al., 2019) while open-sea basins could have been still active in the south (Perón Orrillo et al., 2019). Just after about 485 Ma, the high metamorphic thermal regime of a thinned lithosphere dominates along the entire backarc (Büttner et al., 2005; Larrovere et al., 2011; Carugno Durán and Ortiz Suárez, 2012; Finch et al., 2017; among other).

Within the Sierra de Famatina between 27° to 30° S, thick supra-crustal successions represent sedimentary filling of backarc and intra-arc basins that opened contorting the Gondwana margin. Astini (2003) and Mángano et al. (2003) correlated the incomplete stratigraphic sections at a regional scale and provided a comprehensive picture of the depositional evolution of Famatinian sedimentary successions. A paleontological and paleogeographical perspective of the fossil record is in numerous studies (Aceñolaza and Toselli, 1977; Vaccari and Waisfeld, 1993; Vaccari et al., 1993; Benedetto, 1994; among others). Fig. 1 illustrates the geographic location of the type localities of Lower-Middle Ordovician volcano-sedimentary successions. The well-known stratigraphic profiles are in the northern Sierra de Famatina at Chaschuil Valley, along the western border of Famatina at Cuchilla Negra, Chuschín and Bordo Atravesado; and on the eastern side of the Sierra de Famatina along Cachiyuyo River, Cerro Negro and Volcancito Valley (Esteban, 1993; Mángano and Buatois, 1996, 1997; Astini, 1998; Mángano et al., 2003; Astini and Dávila, 2004; Armas et al., 2016; among several others). A separate belt of Lower-Middle Ordovician strata, which re-crystallized at the thermal aureole of plutonic batholiths on the eastern border of Sierra de Velasco, is grouped in La Cébila metamorphic complex (Verdecchia et al., 2011). La Cébila complex is singular as preserves both original sedimentary structures with fossil stratum but recrystallized under amphibolite and greenschist facies metamorphism (Verdecchia et al., 2007).

Every volcano-sedimentary succession consists of a varied combination of siliciclastic, epiclastic, volcaniclastic, and volcanic rocks of Lower and Middle Ordovician age (Fig. 2a and b). The reconstruction of the Famatinian stratigraphy suggests that the sedimentary process initiated at the uppermost Cambrian, and filled an outer marine shelf (Esteban, 1993). The earliest stage is in the Volcancito Formation that deposited unconformably overlying already folded Middle - Upper Cambrian turbidites (Negro Peinado Formation) but predating the onset of arc-related magmatism (Turner, 1960; Esteban, 1993; Astini, 1998; Candiani et al., 2011). Drowning of the marine shelf occurred during the lowest Ordovician and led to a prevailing of deep water environments (Astini, 1998; Esteban, 2002; Mángano et al., 2003). Late

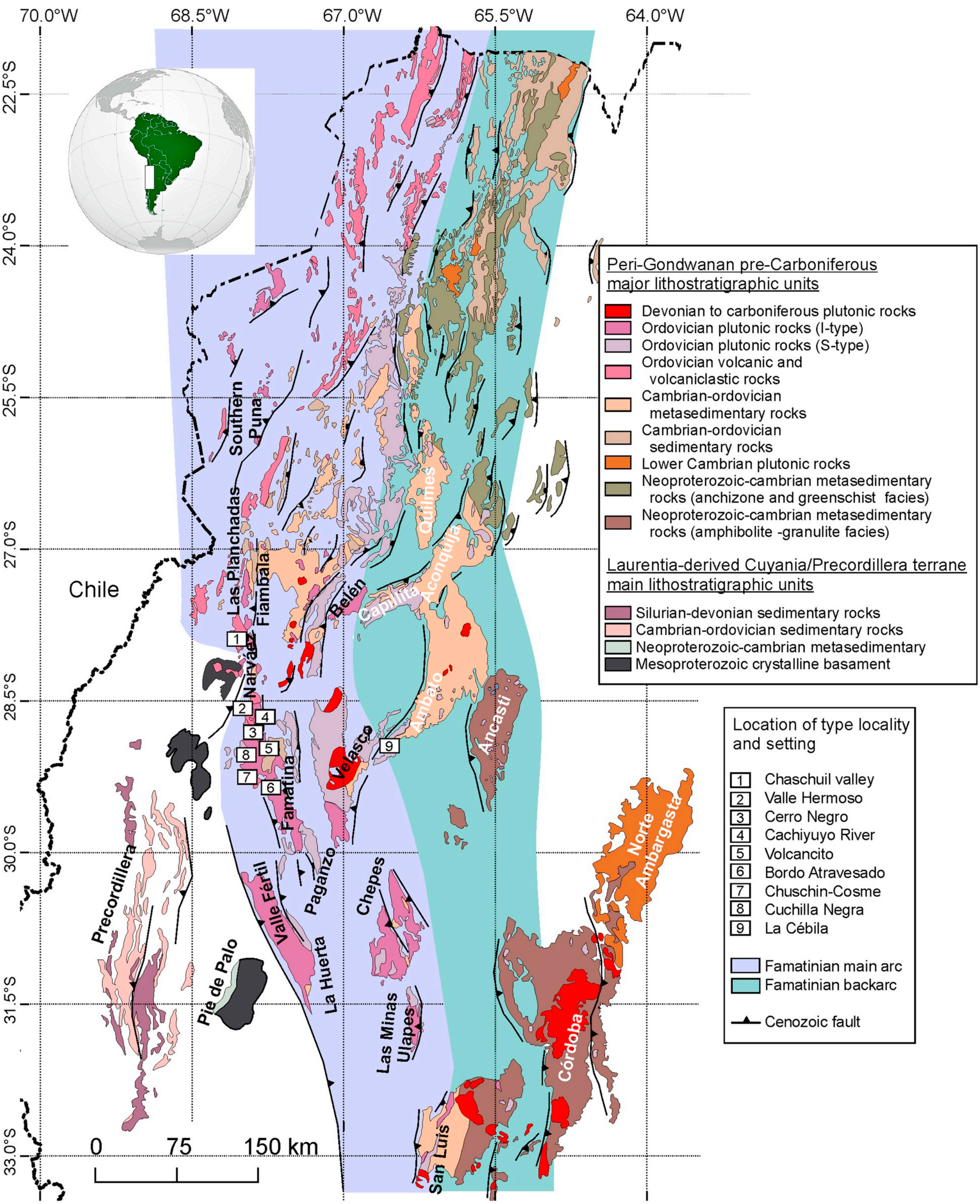

Fig. 1. Generalized geological map of the Famatinian arc in central and northwestern Argentina, showing lithostratigraphic units that are older than the Pennsylvanian epoch. The inset shows the location of the map in South America.

Tremadocian and early Floian deep shelf strata that comprise volcanic tuff in the Bordo Atravesado Formation and volcanic lava flow in the Cerro Tocino Formation record the first evidence for arc-related magmatism (Astini, 1998; Mángano et al., 2003; Candiani et al., 2011). Stratigraphic section at Cerro Negro in the eastern of the Sierra de Famatina also preserves early Famatinian eruptive products within the 120-m-thick black shales of La Alumbrera Formation (Astini, 1998). The strata resting on La Alumbrera are referred to as Portezuelo de la Minitas Formation and consist of a 1500-m-thick succession of sandstones and mudstones with interlayers of basaltic/andesitic sills (Fig. 2c). These formations correlate with the Famatina Group that is exposed along the Cachiyuyo River (Astini, 1998). The Suri Formation, which is the 1200-m-thick lower formation of the Famatina Group, consists of silicified shales, sandstones with sporadic alternating

Fig. 2. Outcrop photos of the volcano-sedimentary succession in the type localities shown in Fig. 1. **(a)** Basaltic lava flow of the Vuelta de las Tolas member in the Suri Formation at Chaschuil Valley. The interlayered relation between tholeiitic basalts and laminated siltstone, silicified sandstone, and volcaniclastic deposit is related to slope apron deposits and basaltic volcanism (Mángano and Buatois, 1996; Cisterna and Coira, 2014). **(b)** Canalized volcanic breccias with erosive bases on a massive mudstone and siltstone bed in the Vuelta de las Tolas member from the Suri Formation. **(c)** Microgabbroic sill emplaced concordant into a well-graded succession of siltstone and mudstone, which are assigned to the Suri Formation at Valle Hermoso in the western Sierra de Famatina (horse and man for scale). **(d)** Chilled coquina bed found at the boundary between the Suri Formation and a rhyolitic lava dome of the Las Planchadas Formation. **(e)** Field view of the plutonic-to-volcanic transition in the Las Planchadas Formation. Monzogranitic rocks with basaltic dikes occur in the bottom half of the image, whereas stratified crystal-poor rhyolite makes up the upper volcanic cap. **(f and g)** Clean mountains provide an outstanding view of the field relationships between the volcano-sedimentary Suri Formation and the intrusive plutonic-volcanic lithostratigraphic units of Las Planchadas within the Chaschuil Valley. **(f)** Crosscutting intrusions of Las Planchadas rhyolitic lava domes (red) into the Suri Formation, which rises to high ridges in the background. **(g)** An isolated relict of the Suri Formation at the roof of Las Planchadas monzogranitic rocks. In the photography, masl denotes meters above sea level.

coquina, and tuff beds. Los Molles Formation is the upper section of the Famatina Group, rests conformably overlying the Suri Formation, and consists of sandstones, siltstones, breccias, and volcaniclastic rocks (Astini and Benedetto, 1996; Astini, 1998, 2003). The characteristic stratigraphy of the Famatina Group indicates progradational backarc and intra-arc apron locally overprinted by growth and collapse of volcanic edifice (Astini, 1998; Mángano et al., 2003).

At the Chaschuil Valley, the Suri Formation comprises cross-bedding sandstone, silicified siltstones, massive black shales, and coquina interbedded with layers of matrix-supported volcaniclastic breccias (Fig. 2d). The sedimentary environment corresponds to volcaniclastic mass flow and storm deposition coupled with suspension fall-out around volcanic centers (Mángano and Buatois, 1996). The Suri Formation at the Chaschuil Valley includes variations from deep marine through inner-shelf to lower-shoreface environment. The Lower - Middle Ordovician volcano-sedimentary successions in the Chaschuil Valley were assigned equivalent to the Suri Formation exposed in its type locality along the Cachiyuyo River (Turner, 1960). However, Mángano and Buatois (1996, 1997) and Cisterna and Coira (2014) revealed notable differences between the stratigraphic columns of the Chaschuil Valley and those exposed at the Cachiyuyo River.

At a mature arc stage, plutonic rocks of batholithic dimensions intruded into the volcano-sedimentary successions and caused thermal aureole metamorphism (Cisterna, 1992; Pankhurst et al., 2000; Alasino et al., 2014). While it is difficult to evaluate the masses of Cambrian turbidite strata and early Ordovician volcano-sedimentary successions cannibalized by the growth of plutonic batholith, what is clear is that the batholith either stopped under the Cambrian turbidites or reached sub-volcanic levels intruding into the epizonal crust (Fig. 2e; Cisterna, 1992; Candiani et al., 2011). Several well-exposed examples of plutonic intrusion into the volcano-sedimentary succession are in the Sierra de Famatina. The contact between the Nuñorco batholith and the overlying volcano-sedimentary units of Cuchilla Negra and Chuschín formations is intrusive and exhibits thermal metamorphism over a wide marginal zone of the host rock (Dahlquist et al., 2008; Alasino et al., 2014; Armas et al., 2018). At the Chaschuil Valley, the volcano-sedimentary successions of the Suri Formation are thermally modified and hydrothermally altered at their basal contact with granitic and rhyolitic rocks of Las Planchadas Formation (Fig. 2f–g).

The volcano-sedimentary successions preserve a progressive transformation from a neutral arc setting to tectonic contraction related to foreland development over some time in the late Dapigian to

Darriwilian (Astini and Dávila, 2004). The first record of convergent stress is an angular unconformity that overlies the Famatina Group and underlies the Cerro Morado Group (Astini, 1998). The Cerro Morado Group is a succession of two contiguous formations. The stratigraphically lower referred to as El Portillo Formation is a 560-m-thick package of rhyolitic and dacitic volcanic deposits comprising ignimbrite, lava flow, and autobreccias (Astini and Dávila, 2004). La Escondida Formation rests unconformably on El Portillo Formation and consists of siliciclastic deposits of sandstones, conglomerates, wackes, and shales, with interlayer of tuff and ignimbrite. La Escondida Formation is a Middle Ordovician shallow marine sequence of alternating sandstone and siltstone deposited in the intertidal zone (Candiani et al., 2011).

La Aguadita Formation is both the last Ordovician lithostratigraphic unit in the eastern Sierra de Famatina and the first to fill of post-magmatic and syn-orogenic strata (Astini, 2003). La Aguadita Formation is a poorly exposed siliciclastic succession of coarse-grained arkose and sandstone, with interlayer of subordinate siltstone (Candiani et al., 2011). Although, the age of La Aguadita deposition remains unconstrained, its sedimentary detritus reflects tectonic unroofing of Ordovician plutonic rocks accompanied by folding and thrusting of Ordovician volcano-sedimentary units (Astini and Dávila, 2004).

2.2. Geobarometric results over the Famatinian arc: estimates of crust exhumation

Large-scale three-dimensional (3D) reconstruction is often-used to working out models synthesizing the growth, accretion, and exhumation of arc crustal sections (Saleeby, 1990; Jagoutz, 2014; DeBari and Greene, 2011; Petterson, 2018). Several works have provided data and developed ideas that are useful to estimations of crustal thickness, among which some reconstructed the backarc (Hauzenberger et al., 2001; Büttner et al., 2005; Larrovere et al., 2011; Carugno Durán and Ortiz Suárez, 2012; Finch et al., 2017; among others) and others the plutonic arc (Dahlquist et al., 2005; Otamendi et al., 2008; Gallien et al., 2010; Tibaldi et al., 2013; Camilletti et al., 2020). These studies used metamorphic petrology information and structural geology data to deconstruct paleodepth of the Ordovician metasedimentary sequence using their peak metamorphic pressures.

Accurate geobarometric estimates calculated with low-variance metasedimentary mineral assemblage provides a reference for retrieving paleodepths across the Famatinian arc crust (extended data for Fig. 3 are presented in appendix S1). These data allow drawing superimposed geobarometric isobars on a schematic geological map of the Famatinian arc (Fig. 3). The isobars on the map show the main features of the Famatinian arc as exhumed today that are: 1) pressures decrease northwards along any given meridian; 2) latitudinal changes of pressures vary along the arc; 3) the highest pressures border the Cuyania-Famatinian suture (i.e., Bermejo – Desaguadero lineament); 4) a modest exhumation spreads over the Puna, the Cordillera Oriental, and along the Sierra de Famatina; 5) the paleopressures vary little over a region interpreted to be backarc exposure; 6) a low-pressure window, which occurs sandwiched between the plutonic batholiths and thick backarc metasedimentary sequences, is where shelly fauna of the Lower Ordovician occurs in greenschist-facies metasedimentary rocks (Verdecchia et al., 2007).

Much of what is considered backarc spanning the eastern belt of the Famatinian arc is exposed at > 5 kbar. In general, any latitudinal paleopressure gradient shows that backarc sections are exhumed from deeper depths than that of the adjacent plutonic batholiths (Fig. 3). The lowest paleopressure of < 2 kbar are found over large parts of the Sierra de Famatina and are prevalent northward of latitude 27° S. Particularly, little and homogenous exhumation is documented over the central part of Sierra de Famatina and only exposes batholithic roofs, subvolcanic systems, and volcano-sedimentary sequences (see section 2.1.).

The N-S transverse from the Sierra de Valle Fértil-La Huerta to the northern Sierra de Famatina offers a continuous gradient in paleodepths. Along this segment of the Famatinian arc, the metamorphic (re) crystallization pressures decrease from the mafic cumulate sequences (7–8 kbar) to relatively shallow-level plutonic batholith within a distance of 450 km (Fig. 3; Tibaldi et al., 2013). To the north and along the same segment is the exposure of the Ordovician paleosurface in the volcano-sedimentary sequences at the Chaschuil Valley (Figs. 1 and 2). This along-strike arc segment is used below to observe magmatic timings and geochemical stratification.

Prominent gradients of exposed paleodepths are spatially related to crustal scales shear zones that are described in section 2.4. West-side-up movement along ductile-brittle shear zones explains another paleopressure bound within the Sierra de Velasco (López and Toselli, 1993; Rossi et al., 2005). Conversely, east-side-up shear of the Tinogasta-Pituil-Antinaco (TIPA) matches deep level exposures on the western side of sierras Velasco and Fiambalá (López and Toselli, 1993; Höckenreiner et al., 2003). Another case is decreasing paleopressures from 8 kbar to 5 kbar in the Sierra de Valle Fértil–La Huerta, where westward thrusting, decoupled uplift, and eastward tilting in the ramifications of a shear zone are considered to explain the gradient of paleopressure across this mountain range (Cristofolini et al., 2014; Camilletti et al., 2020).

The first order characteristic of the Famatinian arc is generalized northward shallower paleodepth of exhumation (Fig. 3). This geological feature might be erroneously related to the Pampean flat-slab segment subduction of the Nazca plate beneath South America. For this reason, below, we discuss the reasons why a Paleozoic continent-arc collision orogeny better accounts for the differential exhumation of the Famatinian arc.

2.3. Geochronological and geochemical stratigraphy of the Famatinian arc

Integration of the geochronological data from literature hints the Famatinian arc formed an entirely synchronous petrological system (Fig. 4; extended data for Fig. 4 in appendix S1). However, the Famatinian arc is not an ideal vertical column through the arc crust, instead, it corresponds to a spatial and temporal continuity along and across the arc. The exposed geology can be the fundamental basis for assessing important issues such as 1) petrological and chemical stratification of the arc crust, 2) internal architecture and its correlations with ancient and active arcs (Tibaldi et al., 2013), 3) magma production rates in the Famatinian arc (Ducea et al., 2017), and 4) petrological mechanism as fingerprints of mantle source *versus* intracrustal differentiation processes (Rapela et al., 2018).

The distribution of ages along and across the Famatinian arc spreads over a period of about 20 Ma (491–465 Ma; see Rapela et al., 2018). However, a great mass of the magmatic crust was produced during a *ca.* 10 Ma period (474–467 Ma) of the Lower - Middle Ordovician (Ducea et al., 2017). Tens of crystallization ages through the arc crust show a continuous rather than punctuated magmatic evolution (Fig. 4). The continuous temporal record from the lowest exposed levels to the volcanic successions suggests a single-cycle episode that grew up a high-fluxes magmatic stage (Ducea et al., 2010, 2017; Rapela et al., 2018). Two aspects of age distribution are significant, these are: 1) the batholiths of the sierras de Chepes and Las Minas-Ulapes predated the time of generation of most other plutonic batholiths, and 2) the end of the magmatic cycle is rapid and synchronous throughout the magmatic column, at the Middle Ordovician (*ca.* 465 Ma). That means, the magmatic front migrated westward (outboard) during the arc stage, and magmatism suddenly stopped when the magmatic arc began evolving through contractional stress and topographic uplift (Astini and Dávila, 2004; Cristofolini et al., 2014).

Published chemical data are useful to unravel the pressure dependence of the magmatic record (Fig. 5). First, it should be noted that the available geochronology is inexact to correlate magmatic tempos at a

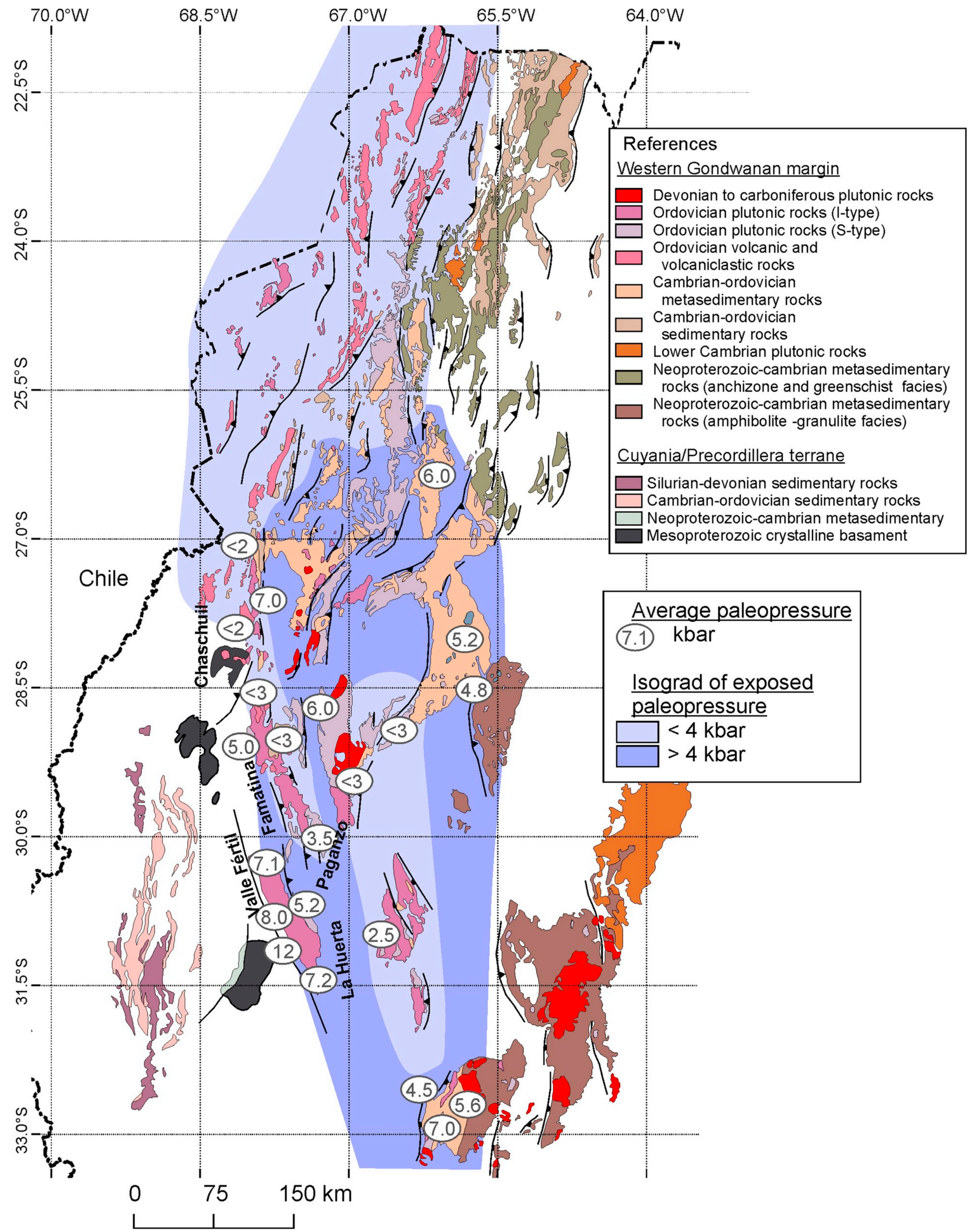

Fig. 3. Regional variations of crystallization pressure in the Famatinian arc estimated performing barometry with mineral assemblages of metasedimentary rocks. Note high pressures (> 4 kbar) dominate in the southern and west-central part of the Famatinian arc, whereas low pressures (< 4 kbar) span to the north of latitude 26° S and over the Sierra de Famatina, Sierra de Chepes and Sierra de Las Minas-Ulapes.

temporal scale lower than about a few million years. Therefore, the following presentation addresses the time-integrated compositional variations throughout the exposed crust. At a glance, the first order petrological and chemical stratification of the Paleozoic Famatinian arc resembles that of the upper 30 km of the Kohistan arc (Jagoutz, 2010, 2014; Jagoutz et al., 2011). However, except for strongly incompatible elements, the chemical column is not strongly stratified (Fig. 5). The lithological diversity spans the compositional range from ultramafic/

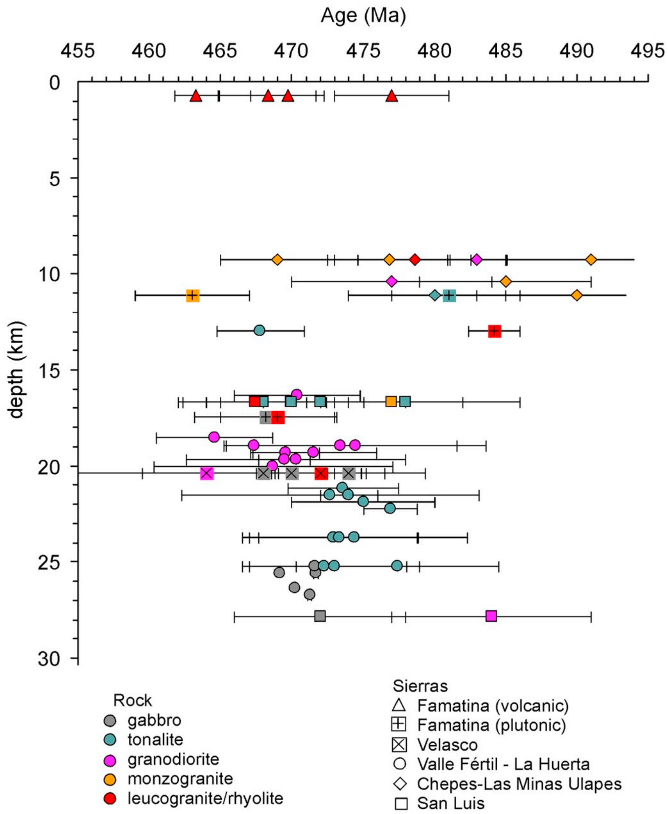

Fig. 4. Crystallization U-Pb ages projected onto an averaged 1-D depth section using paleopressure estimates shown in Fig. 3 and described in the text. All are U-Pb zircon crystallization ages of which the original papers provide details about equipment, methodology, accuracy, and error. Sources of ages are given in Appendix S1.

mafic plutonic rocks to felsic leucogranites. Although, mafic rocks dominate the lower levels and granitic/rhyolitic rocks prevail over the shallow crust, at all the exposed crustal levels the igneous sequence shows an ample compositional variability of SiO_2 from ≤49 wt % to > 73 wt % (Fig. 5a). Petrologically significant elemental ratios broadly follow the variation of SiO_2, for instance FeO*/MgO ratios range equally at every crustal depth and across the crustal levels (Fig. 5b). This is also valid for major oxides such as CaO (Fig. 5c) and alumina saturation index (not shown). Opposite to the other oxides, K_2O displays progressive enrichment upward in the crustal column (Fig. 5d).

According to the chemical criteria of Jagoutz et al. (2011), most of the mafic rocks in the lower crust are chemically cumulates, but excluding the discrete ultramafic-mafic layered bodies, the plutonic mafic rocks show re-equilibrated mineral assemblages and metamorphic structures. The majority of the rocks with a major oxide composition of primitive igneous chemistry ($48 < SiO_2 < 52$ wt %, and MgO/MgO + FeO* ratio > 0.65 or FeO*/MgO < 0.95) are found in the deep crust (Fig. 5a and b). Even more significant is that integrating the exposed paleodepths, mafic rocks ($SiO_2 < 52$ wt %) are one-third of the magmatic sequence. Typical intermediate and silicic rocks form the thick (ca. 15 km) middle crust (Camilletti et al., 2020). The middle crust is stratified into a tonalitic lower part and granodioritic and monzogranitic upper levels, but the middle-crustal batholiths consist of an ample spectrum of plutonic rocks (Saavedra et al., 1998; Pankhurst et al., 1998, 2000; Otamendi et al., 2012; Alasino et al., 2016).

The volcanic sequence comprises bimodal basaltic–rhyolitic series, accompanied by subordinate andesites and rhyodacites (Fig. 5; see Mannheim, 1993). The mafic volcanic rocks display subalkaline and tholeiitic characteristics (Mannheim, 1993; Cisterna and Coira, 2014). The high MgO/MgO + FeO* ratio (0.55–0.63) together with Cr and Ni contents of the Famatinian basalts indicate that basaltic volcanism was produced by little fractionated melts derived from deep-seated primitive sources (Mannheim, 1993; Toselli et al., 1990). The rhyolites in the Famatinian arc are characterized by high SiO_2 contents ranging from 70 wt % to 79 wt % (Fig. 5a). Predominant rhyolite has high total alkali ($Na_2O + K_2O > 4.5$ wt %) abundances, is weakly peraluminous (molar $Al_2O_3/(CaO + Na_2O + K_2O)$ values of 1.0–1.3), and shows a smooth chondrite-normalized REE pattern with marked negative Eu anomaly but variably fractionated La_N/Yb_N ratio (Mannheim, 1993; Armas et al., 2018). Mannheim (1993) uses elemental geochemistry to reveal the absence of genetic relationship between basalt and rhyolites over the Famatinian arc. Importantly, the volcanic products largely reflect the chemical diversity of the underlying plutonic column (Fig. 5).

2.4. Shear zones of the Famatinian orogen

Numerous articles dealt with shear zones in the Famatinian arc – orogenic system (Whitmeyer and Simpson, 2004; Castro de Machuca et al., 2008; Cristofolini et al., 2014; Larrovere et al., 2017; Christiansen et al., 2019; and references therein). The following is a brief introduction to the shear zones of interest. At arc scale, the prominent pattern of deformation is amphibolite-to greenschist-facies temperature shearing that formed after the plutonic and synmagmatic metamorphosed rocks had mostly crystallized. Mylonite and cataclastic-series rocks are dominant in NNW-striking and variably-dipping shear zones at a regional scale (Fig. 6). Here, the focus is on showing the geographic distribution of major shear zones that accommodated the uplift of the Lower and Middle Ordovician crystalline crust between 27° and 33° S (extended data for Fig. 6 in appendix S2). Major shear zones relevant to our discussion are described in order from west to east: 1) Valle Fértil – La Huerta shear zone; 2) Cordón de la Cumbre, Chuschín and Paganzo shear zones; 3) the TIPA shear zone; 4) the shear system within the Sierra de San Luis and its northward extension into the sierras Chepes and Las Minas, 5) La Chilca shear zone; and 6) the Guacha Corral - Pachango shear zone.

The western Sierra de Valle Fértil – La Huerta is comprised of an anastomosing network of separate shear zones. NNW-trending and steeply dipping mylonites dominate over a long central segment. Locally, in the northern section mylonites are N-trending and moderately dipping (40° – 55°) to the east, whereas on the western border mylonites exhibit moderate to steep (65° to > 80°) dips to the west. Westward-directed dip-slip movement explains the uplift of several kilometers of the Middle Ordovician arc crust in the Valle Fértil – La Huerta shear zone (Gallien et al., 2010; Castro de Machuca et al., 2008, 2012; Cristofolini et al., 2014).

A discontinuously exposed but aligned shear belt extends from the southern Sierra de Paganzo through the southwestern foothills to the northern ranges of the Sierra de Famatina (Saal, 1993; Martino and Astini, 1998; Conci et al., 2001). The Cordón de la Cumbre belt is a 500-m-wide, NNW-SSE striking and W-dipping (65°) ductile shear zone that extends along the high topography of the Sierra de Famatina (Martino and Astini, 1998). This belt is one of the few E-verging shear zones, and it juxtaposes shallow plutonic batholiths over complementary but strained volcano-sedimentary successions (Astini and Dávila, 2004). On the western Famatina foothills, the Chuschín shear zone is an up to 200-m-wide belt in the Middle Ordovician volcano-sedimentary succession. The Chuschín zone is NNW-SSE striking and steeply dipping (75°) to the east, and shows W-directed reverse displacement with a minor sinistral component. Nucleated on plutonic and metamorphic rocks, the Paganzo shear zone shows the same tectonic features as the Chuschín zone. The exposure of the Paganzo shear belt, with a length of 40 km and a width of up to 500 m, is one of a large shear zone in the Sierra de Famatina (Saal, 1993; López and Toselli, 1993).

A long dendritic belt, TIPA, of mylonite and ultramylonite rocks,

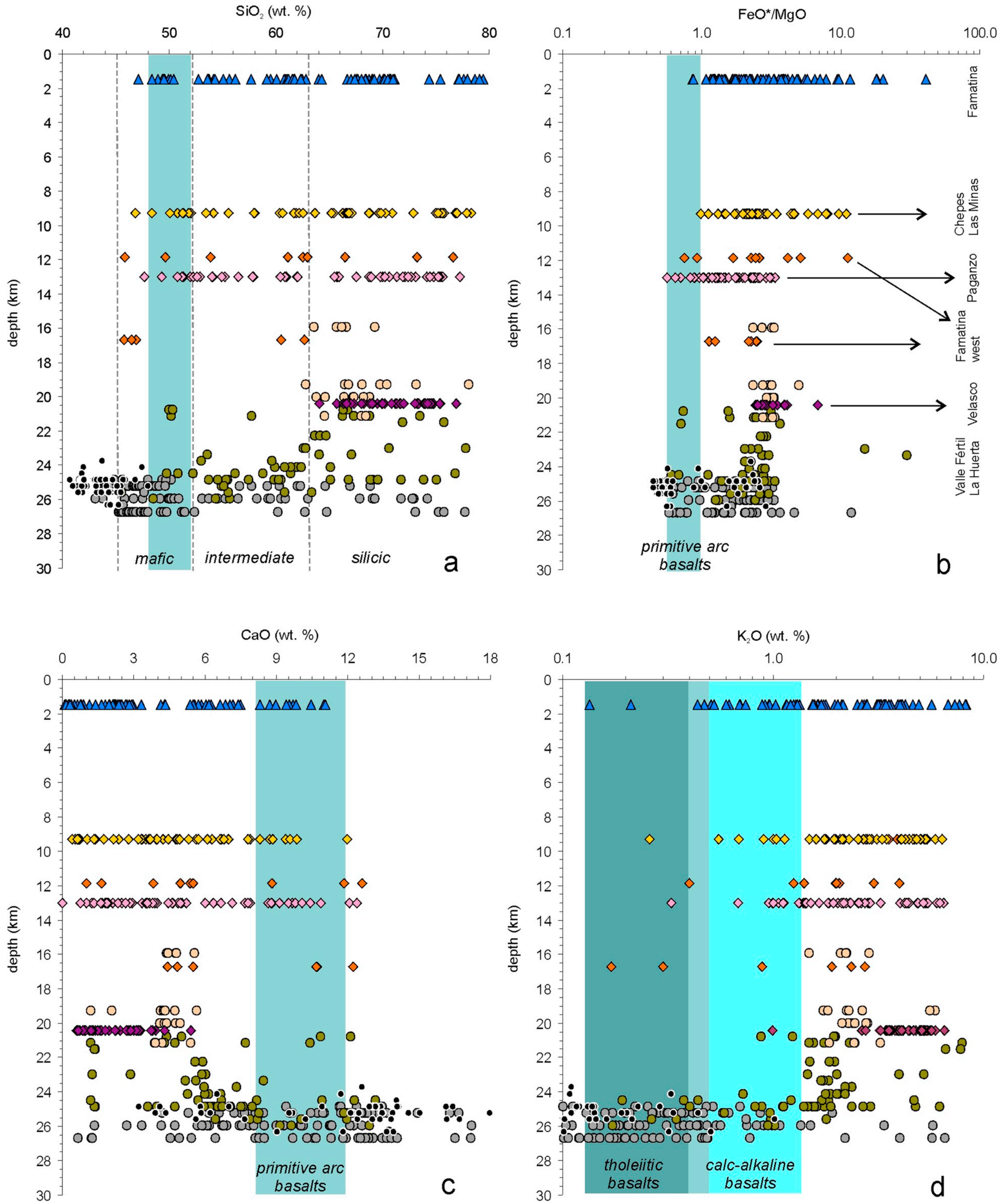

Fig. 5. Diagrams that project whole-rock composition against crystallization depth using the paleopressure estimates of Fig. 3. The range of major oxides in primitive melts of subduction zones is after Schmidt and Jagoutz (2017). The lithostratigraphic units in the Sierra de Valle Fértil-La Huerta are illustrated by different color: black and grey for cumulate and non-cumulate rocks, respectively, of the mafic unit; dark green for plutonic rocks of the intermediate unit; and light orange for rocks of the silicic unit. Plutonic rocks from each Famatinian locality are distinguished by varying the color of filled diamonds (panel b). Blue-colored triangles are volcanic rocks taken over the Sierra de Famatina. The sources of whole-rock analyses are given in Appendix S1. (For interpretation of the references to color in this figure legend, the reader is referred to the Web version of this article.)

which formed upon the reworking of Lower Ordovician granitoids, occurs as NNW–SSE-trending ductile shear zones along sierras Velasco, Paimán, Copacabana, and Fiambalá (López and Toselli, 1993; Höckenreiner et al., 2003). Most of the shear zone is ENE-dipping with moderate to steep plunging (45°-66°). The zone is WSW-verging with a dominant reverse sense of movement accommodating east onto west thrusting (Fig. 6). A subordinate along-strike shearing of dextral displacement irregularly developed along the northern segment of the

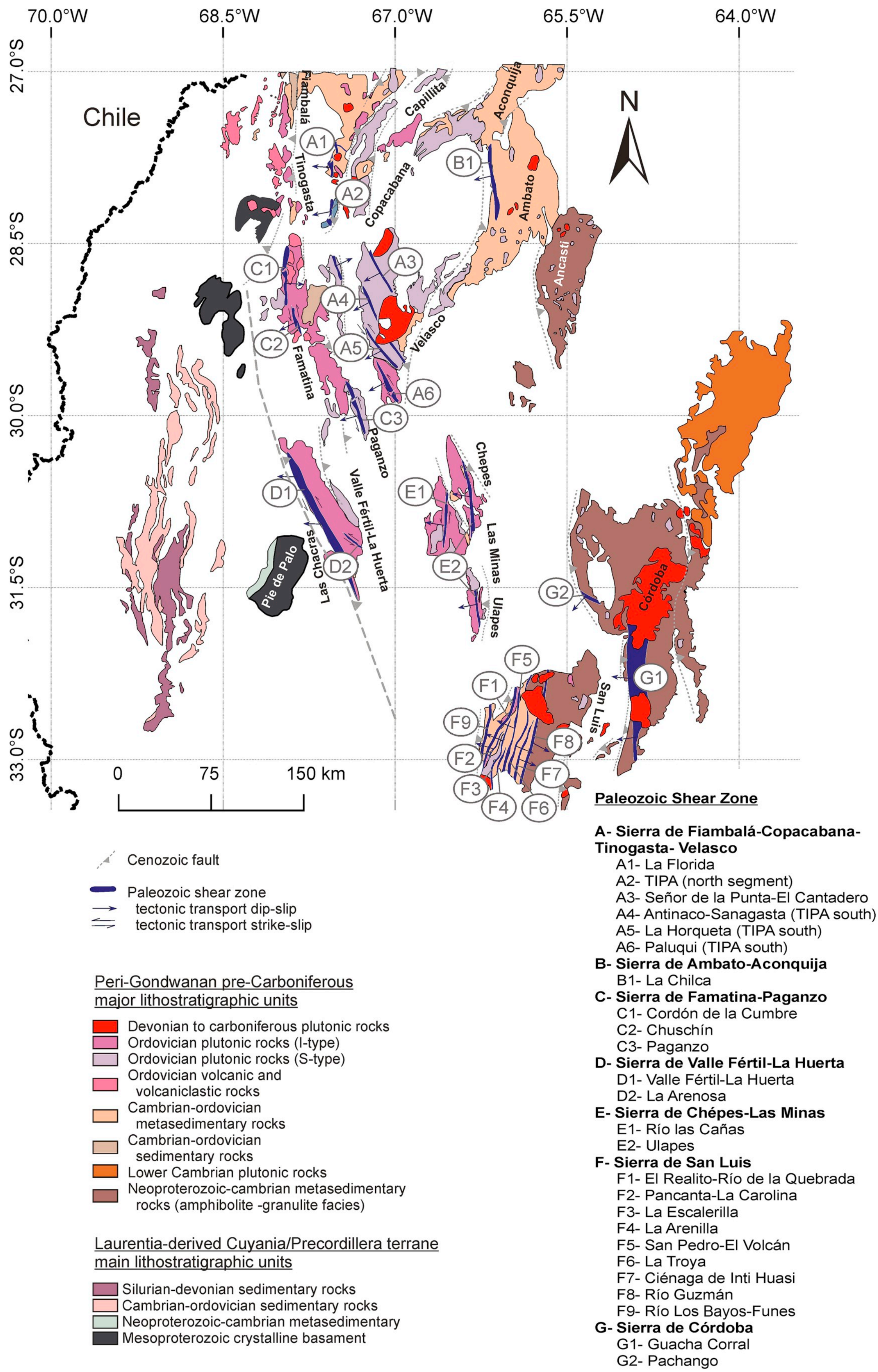

Fig. 6. Geological map of the Famatinian arc that shows the location of the major shear zones between latitudes 27° and 33° S. Appendix S2 describes the characteristics of the Famatinian shear zones discussed in the text.

TIPA zone. Overall, the TIPA shear system separates crustal scale segments showing different paleodepth of exhumation (Höckenreiner et al., 2003). The dominant dip-slip tectonic transport juxtaposes a high-P block in the east onto a low-P plutonic crust in the west. East of the TIPA zone, the Famatinian arc is strongly deformed and exposes prevailing S-type granites (Sierra de Velasco) and metasedimentary gneisses and migmatites locally intruded by mafic layered bodies (Sierra de Fiambalá). On the opposite western side of the TIPA zone, the Famatinian batholiths and their volcanic expression have widespread exposure (Fig. 6).

The shear system of the Sierra de San Luis comprises, at least, nine discrete zones of definable width and broadly NNE-SSW-trending subvertical mylonitic foliation (von Gosen and Prozzi, 1998; Whitmeyer and Simpson, 2004; Morosini et al., 2014). On the western part of the Sierra de San Luis, the shear zones are curved and show a large-scale anastomosed pattern (Fig. 6). As a whole set, the shear system juxtaposes granulite-facies onto amphibolite- and greenschist-facies lithostratigraphic units and causes an inverted metamorphic gradient (Ortiz Suárez and Casquet, 2005). West-verging shear zones are present on the west side of the San Luis shear system, whereas they are E-verging on the east side. However, irrespective of verging orientation, all shear zones present prevailing reverse tectonic transport with subordinate sinistral displacement and local dextral motion (von Gosen and Prozzi, 1998; Christiansen et al., 2019).

Within the sierras Chepes and Las Minas-Ulapes, shearing frequently nucleated in plutonic rocks, and rarely propagated into metasedimentary rocks (Sims et al., 1998; Simpson et al., 2003). The southern Las Minas shear zone is a 1-km-wide branching mylonitic belt which is N-S-trending and steeply dipping to the east. The northern segment of the shear zone located in Sierra de Chepes is trending NNE-SSW and steeply-dipping to both the east and west (70°–85°). Over the sierras Chepes and Las Minas, the mylonitic stretching lineation is moderately dipping to the east suggesting reverse W-directed tectonic transport (Sims et al., 1998; Simpson et al., 2003).

At the NE corner of the region being discussed sits the La Chilca shear zone (Larrovere et al., 2017). This shear zone, which is exposed straddling the border between the sierras Aconquija and Ambato, displays a 24-km-long and up to 4-km-wide belt composed of mylonites and protomylonites (Fig. 6). Mylonitic foliation is NNW-SSE striking and dips moderately to the east. Within a folded mylonitic belt, shear sense criteria show bulk kinematics of reverse dip-slip movement with top-to-SW tectonic transport (Larrovere et al., 2019).

The Guacha Corral-Pachango shear zone is briefly described here because its key tectonic activity is coeval with Famatinian events, but it differs from others in that is nucleated on Lower Cambrian metamorphic rocks (Martino, 2003; Whitmeyer and Simpson, 2003; Demartis et al., 2017; Semenov et al., 2019). The Guacha Corral-Pachango shear zone is both one of the widest and the easternmost records of Cambrian to Devonian W-directed thrust tectonic (Martino, 2003). Gneisses and migmatites with gradual changes to N-S trending, E-dipping mylonites comprise this shear zone. Original metasedimentary rocks show tectonic fabrics over the entire mylonite series recording strong strain partitioning inside the zone (Demartis et al., 2017). Mylonitic mineral assemblages are of amphibolite-to greenschist-facies and retrogression correlates with shear strain concentration (Martino, 2003; Whitmeyer and Simpson, 2003; Semenov et al., 2019).

3. Results and interpretations

3.1. Inferred magmatic processes in the Famatinian arc

A roughly 30-km-thick magmatic system, including more than one-third of a mafic component plus intermediate to silicic plutonic and volcanic rocks, entails specific sources and differentiation phenomena (Fig. 5; see Jagoutz, 2010). Our approach here proposes that a general petrological model has to pass the test of explaining both the relative abundance and the variation range of major elements (section 2.3.). Geochemical modeling based on trace elements and isotopes could refine the petrogenetic model, but the improvement should preserve the conclusion reached using major elements. The starting point is that mantle-derived mafic magmas ascending from the mantle-crustal boundary are the driving power of crustal magmatic systems (Hildreth and Moorbath, 1988; DeBari, 1997; Annen and Sparks, 2002). Good evidence for the composition of primitive magmas is within the Sierra de Valle Fértil – La Huerta (Otamendi et al., 2009; Walker et al., 2015). Primitive magmas that fed the base of the Famatinian arc are in the range of low-K medium-Fe/Mg tholeiitic basalts (e.g., Arculus, 2003; Schmidt and Jagoutz, 2017). Here our interest focuses on two questions: 1) what petrological mechanism does explain the full spectrum of magmatic rocks? and 2) how much cumulate has been extracted from a parental basaltic melt to derive the intermediate and silicic rocks? Indeed, the questions are connected.

As discussed by Walker et al. (2015), stepwise fractional crystallization is important in controlling igneous diversification over the mafic to intermediate transition. Data presented in the literature and shown above, however, indicate that closed-system crystal-liquid fractionation alone cannot account for the entire compositional trend of the Famatinian rocks (Otamendi et al., 2012). The critical question is how to cross the "gabbro barrier" to generate the bulk chemistry of intermediate and silicic rocks (Walker et al., 2015). For qualitative illustration, we use relative and absolute abundances of major oxides in whole rocks associated with the composition of mineral phases giving an adequate record of geochemical variations (Fig. 7). The extraction of Fe-Ti oxides, olivine ($Fo_{83\text{-}80}$), amphibole, and plagioclase ($An_{>80}$) from a primitive mafic magmas (SiO_2 ~49 wt %) drives the increment of SiO_2 over the gabbro to tonalite transition (Fig. 7a). However, crystal fractionation of olivine and accessory Fe-Ti oxide depleted FeO* and MgO while it cannot significantly raise SiO_2 content of the evolving magma (Fig. 7a–b). Crystal fractionation of plagioclase may counterbalance the effect of olivine plus oxides, and hence an early crystallizing assemblage combining these three phases would drive the compositional trend of rocks. Alternatively, an early crystallizing assemblage dominated by amphibole can explain the Harker-type variation of FeO* and MgO. However, every given assemblage of crystallizing minerals moves the content of SiO_2 less than 5 wt % (Fig. 7a–b). A realistic model for increasing SiO_2 over the gabbro to tonalite transitions faces the other two major dilemmas. One is that the peritectic crystallization of orthopyroxene from reactive olivine buffers the variation of SiO_2 in an evolving magma (Bowen and Schairer, 1935). Another is that the prolific extraction of amphibole precludes increasing potassium in the residual melts (Fig. 7c). Certainly, igneous differentiation passes by the gabbro barrier, but at the cost of retaining a low-K signature. This is in line with fractional crystallization experiments of hydrous magmatic series that showed, over the range of SiO_2 contents from tonalites to granites, the abundance of K_2O would not increase more than 4 times the initial K_2O content of a parental gabbro (Nandedkar et al., 2014; Müntener and Ulmer, 2018). The majority of the intermediate and silicic plutonic rocks have higher K_2O than that generated by closed-system fractional crystallization. The effect of the petrological mechanism on driving chemical evolution is visible in the CaO/Na_2O versus K_2O diagram (Fig. 7d). Plagioclase-dominated crystal extraction governs reduction of CaO/Na_2O ratio from primitive magmas, but neither olivine nor amphibole moves the CaO/Na_2O ratio (Fig. 7e). To a large extent, amphibole and minor oxides accompanied plagioclase in the early crystallizing assemblage (Walker et al., 2015). Closed-system fractional crystallization of mantle-derived melts produced both the magmatic ultramafic-mafic lower crust and derivative melts (Fig. 7a, b and 7e; also see Müntener and Ulmer, 2018). Yet, it is open-system hybridization between mafic magmas and partially molten metasedimentary rocks that causes the high abundance of K_2O of intermediate plutonic rocks (Fig. 7d–e). The strong K_2O enrichment that goes with the exponential fall of CaO/Na_2O ratio is what has been

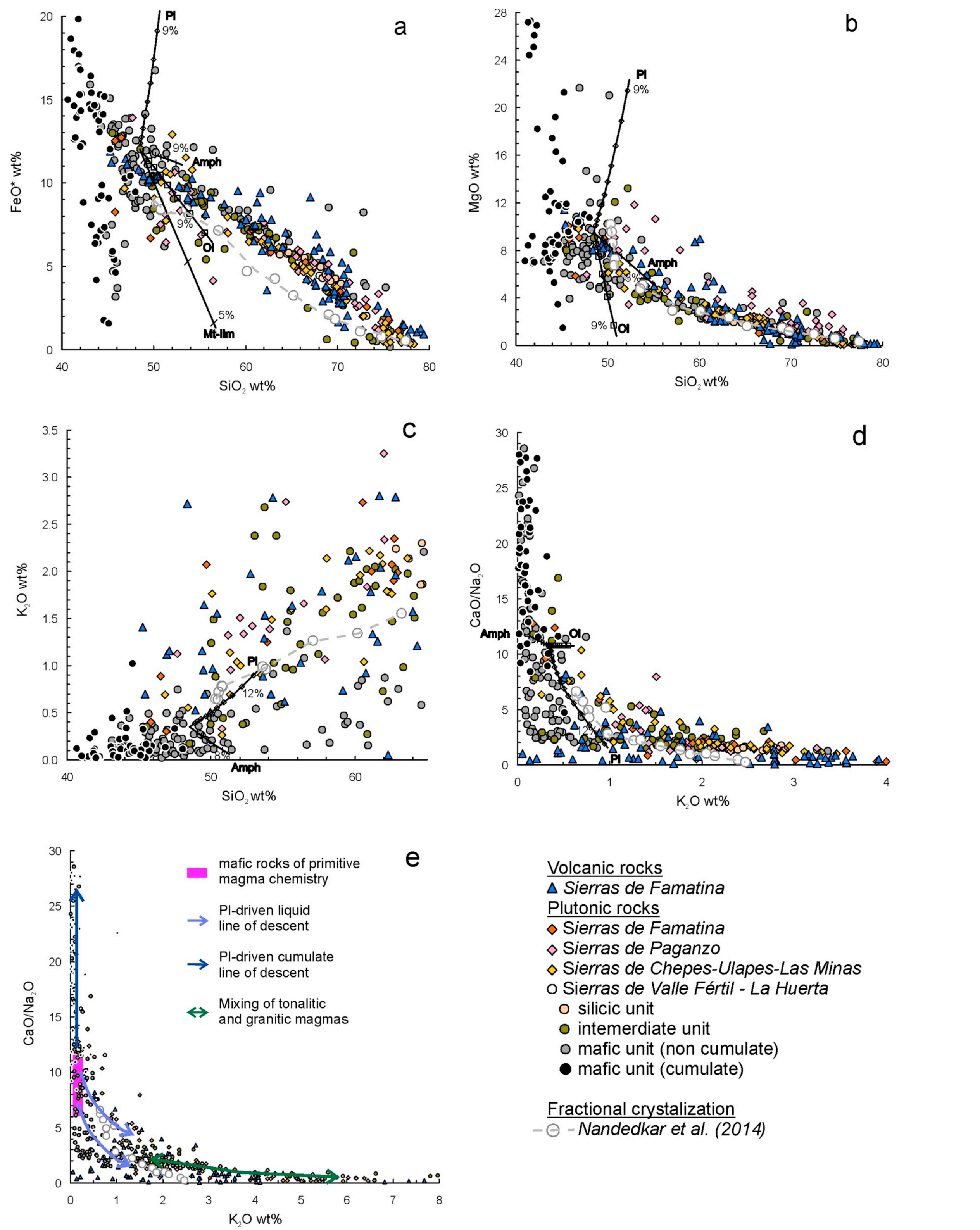

Fig. 7. Harker variation diagrams for whole-rock compositions and mineral vectors. Mineral abbreviation at the arrow's tip explains the compositional trend of every given fractionating mineral. Tick marks on the curves show values of weight percentages of the minerals extracted separated by 1 wt % step. Mineral abbreviations are: Ol for olivine, Pl for plagioclase, Amph for calcic amphibole, and Mt-Ilm for Fe-Ti oxides. The sources of whole-rock analyses are given as supplementary data in Appendix S1.

explained by hybridization between mantle-derived gabbroic to tonalitic magmas and supracrustal-derived (meta)sedimentary materials (Otamendi et al., 2012). At a given SiO_2 content, the K_2O abundance of intermediate and silicic plutonic rocks reflects the extent to which a mantle-derived magma has assimilated pre-existing continental crust. This chemical sensor cannot distinguish the nature of a continental source as either craton-derived sedimentary rocks or ancient lower continental crust yield the same chemical (elemental and isotopic)

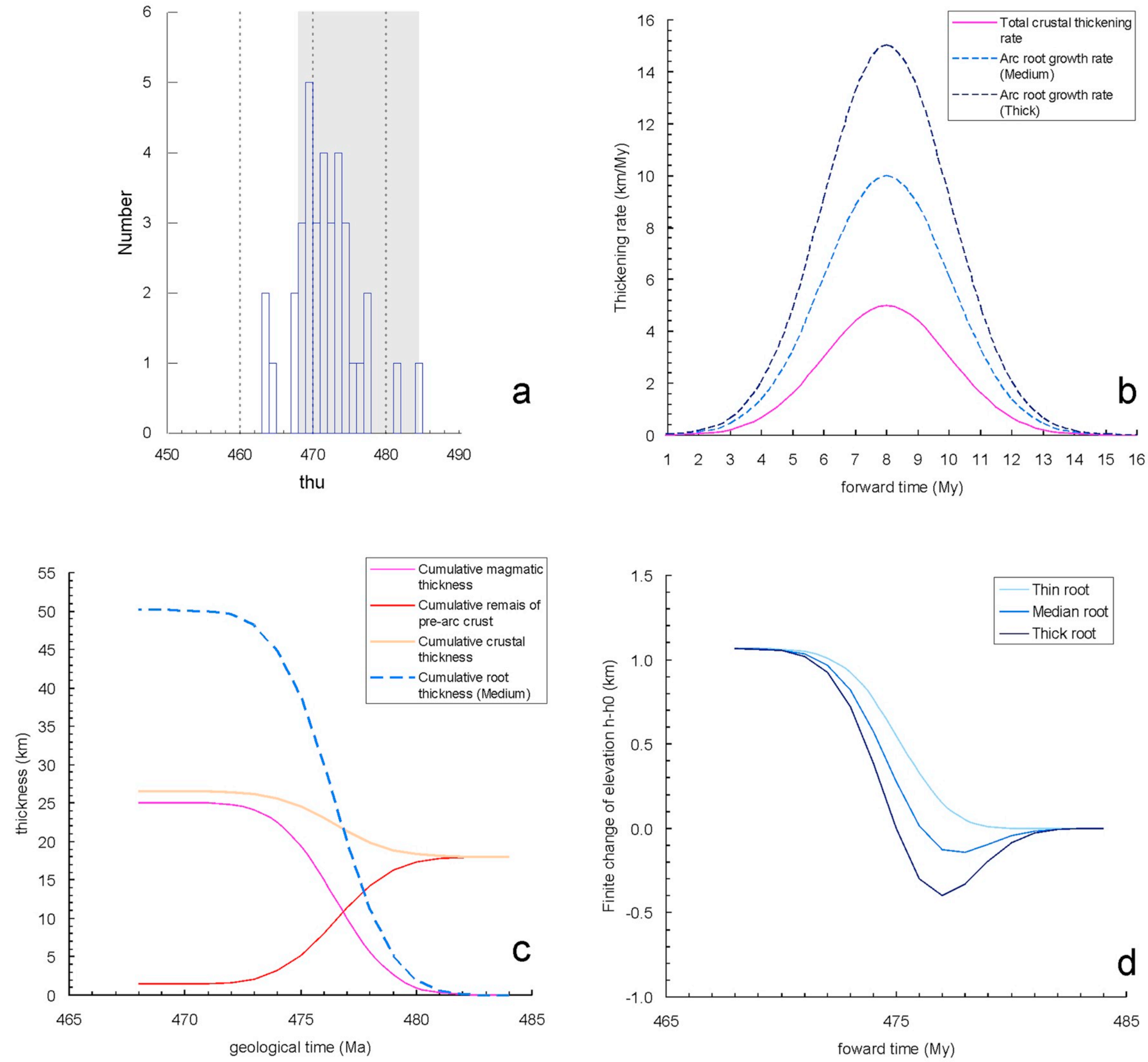

Fig. 8. (a) Histogram of Famatinian ages highlighting the time span of the high-fluxes magmatic episode with a grayed overlaid. (b) Gaussian distribution curves simulating the magmatic rate of crustal and root growths scaled to the total crust thickness (solid line) and arc root growth (broken line). **(c)** Evolution of cumulative crustal and arc root thickness from the onset of Famatinian arc magmatism (485 Ma) to the beginning of collision closure (469 Ma). **(d)** Evolution of elevation (h) from the initial surface elevation (h_o) over the time span of the model. The text describes the conceptual basis for modeling isostacy.

signature (Saleeby, 1990). With this caveat in mind, field-based observations and petrological analyses provided a first answer. Petrological differentiation starts at deep-seated levels where a cumulate line of descent follows a stepwise crystal fractionation chain (Walker et al., 2015). The cumulate pile drains the evolved melts that differentiate and assimilate supracrustal-sourced materials over the entire middle and shallow Famatinian crust (Otamendi et al., 2010; Camilletti et al., 2020).

How much mass of the arc is in the cumulate roots? From different perspectives, the question gives similar answers (Ducea, 2001; Jagoutz, 2010; among others). But, in the case of interest, it poses a simple argument, the mass budget of the petrological process governing the transition from gabbro to tonalite primarily determines the relative mass of cumulate and derivatives (Jagoutz, 2010). In general, ideal *in-situ* equilibrium crystallization does not fractionate the SiO_2 content of the system, whereas perfect fractional crystallization maximizes the effect of crystal-liquid separation on igneous differentiation (Müntener and Ulmer, 2018). Keeping in mind this concept, we have estimated the ratio between cumulate and derivative melt using the composition of natural rocks and their bearing minerals (Camilletti et al., 2020). Our mass balance is consistent with the results of fractionation-crystallization experiment using a wet basaltic parental magma at 7 kbar (Nandedkar et al., 2014; Müntener and Ulmer, 2018). To develop the evolved melts ($52 < SiO_2 < 72$ in wt. %) that construct the intermediate and silicic plutonic sequence, the petrological engine leaves behind nearly one half of the magmatic mass in ultramafic/mafic cumulates (Camilletti et al., 2020). Providentially, the transition from gabbro-dominated to the tonalite-dominated crust, which emplaced at a range of about 26 ± 3 km of paleodepths, is exposed within the Famatinian arc (Tibaldi et al., 2013; Camilletti et al., 2020). It implies that fractionation steps at deeper depths were unable to move out from the ultramafic – mafic compositional system. However, mafic melts emplaced close to the mafic – intermediate transition had MgO/MgO + FeO* ratio of about 0.6 reflecting that their last equilibration lies outside (i.e., above) the peridotitic/piroxenitic asthenospheric mantle (Otamendi et al., 2010; Walker et al., 2015). Deeper than exposed igneous fractionation lowered the MgO/MgO + FeO* ratio, but neither depleted SiO_2 and CaO nor enriched K_2O of the primitive mafic melts that reached the lower and middle crust. The Kohistan arc is unique in showing the arc root (Jagoutz et al., 2011; Bouilhol et al., 2015). In contrast, the deepest exposed paleodepths at the Famatinian arc prevent observing the lithologies found in the Kohistan arc. By analogy, the root of the Famatinian arc may have been an arc cumulate sequence that included ultramafic rocks (harzburgite, dunite, and clinopyroxenite) and garnet- or plagioclase-bearing gabbroic rocks. Immediately the problem arises, how thick the Famatinian arc root was?

3.2. Significance of mass balance and isostasy model on constraining arc construction

Since geology preserves a good record of paleo-elevation of the Famatinian arc from inception to closure (section 2.1.), a simple treatment enables appraising the topographic evolution of the Famatinian arc. The arc construction is constrained using geological information documented along the segment from the Sierra de Valle Fértil – La Huerta to the Chaschuil Valley in the northern Sierra de Famatina (Fig. 1). Topographic changes are treated following the basic principles of isostasy (Lee et al., 2015; Cao and Paterson, 2016). A common assumption is that the lithosphere is in isostatic balance over long enough scales of hot and weak crust (Lee et al., 2015). The isostatic principles obey the general equation:

$$\Delta h(t) = h(t) - h_0 = \left(1 - \frac{\rho_c}{\rho_m}\right)(H(t) - H_0) + \left(1 - \frac{\rho_r}{\rho_m}\right)R(t)$$

Elevation (h) is a function of crust thickness (H) and arc root thickness (R). Before magmatism starts building up an arc crust, the initial conditions are the topographic elevation (h_o) and the crustal thickness (H_0). In the fundamental equation, ρ_m (3.2 gr/cm^3), ρ_c (2.8 gr/cm^3), ρ_r (3.4 gr/cm^3) are densities of the mantle, crust, and arc root, respectively.

Our approach focuses on the magmatic accretion that is one of the three causes affecting elevation and crustal thickness. Active erosion and far-field stress regime are the other two sources modifying crust thickness (Cao and Paterson, 2016). Assuming the absence of deformation is a flaw of isostatic modeling, but pondering crustal strain requires developing a specific survey. However, there are few field data to discuss the significance of bulk arc strain on crustal thickening. In contrast, ignoring the erosion of the arc crust is not a problem of isostatic modeling because the Famatinian volcano-sedimentary successions deposited while volcanic lavas flowed in deep to shallow marine environments (section 2.1.).

Although the age pattern of the Famatinian magmatism approximates a log-normal distribution (Fig. 8a), the magmatic model follows a Gaussian distribution (Fig. 8b), as suggested by Cao and Paterson (2016). The difference between natural and model functions used to describe the dependence of magmatic accretion to time does not influence the result as long as the total volumetric magmatic fluxes fit nature. At any given time after arc inception, the crustal thickness is the difference between the accumulated magmatic additions from the mantle source to the crust reservoirs minus the mass of pre-arc crust recycled to make the magmatic crust (Fig. 8c, also see Ratschbacher et al., 2019). The event of interest began at 485 Ma and ended at 468 (sections 2.1. and 2.2.). This lifespan ranges from the oldest plutonic crystallization in the southern Famatina (MIR1014 of Pankhurst et al., 2000) to the time at which a continent-to-arc collision had begun to close the Famatinian arc (Astini and Dávila, 2004; Cristofolini et al., 2014). The initial condition has a 10-km-thick stacked (supra)crustal accretionary wedge above an 8-km-thick mafic crust (Otamendi et al., 2012). To parameterize arc growth during the magmatic stage, every volumetric fraction of magma added to the crust, averaging at 1.53 km^3/km^2/My during 17 My, includes a fraction (40 %) of recycled pre-arc crust incorporated by assimilation (see section 3.1.). It turns out that the pre-arc crust reduces to less than 10% from its original bulk mass after 15 My of magmatism (Fig. 8c). The projection of composition against depth shows that the fraction of mafic rocks increases and silicic rocks decrease with increasing depth (Fig. 5). However, the model only considers bulk crust thickness as a function of time (Fig. 8c). Furthermore, to simplify the calculation, it is assumed that the density of the crust remains constant. The volumetric arc root construction correlates to the volumetric magmatic fluxes generating new crust (Lee et al., 2015). A critical parameter (γ) of isostatic modeling is the ratio between mass-of-root (R*t*) to the mass of derivative magmatic addition (M*t*). Compared to the background mantle density, the igneous-evolved magmatic addition is positively buoyant, by contrast the cumulate rooted mass is denser and potentially delaminated. Modeling considers three scenarios with γ increasing from 1 (thin root) to 3 (thick root) that is consistent with observations in the Phanerozoic arcs (Cao and Paterson, 2016) and our previous study (Camilletti et al., 2020).

Two observations are targeted in modeling. First, field geology, stratigraphy, paleontology, and geochronology suggest that the Famatinian arc evolved below sea level during the Lower and Middle Ordovician except where the volcanic edifices raised high above their bases (section 2.1.). An inherent inaccuracy in the modeling precludes accounting for global sea-level variations so that the result is a gross approximation at a thickness scale of hundreds of meters. The second observation to model is that, by the end of Famatinian magmatism, the intermediate-silicic plutonic and volcanic crustal column reached a thickness of about 25 km (Tibaldi et al., 2013; Camilletti et al., 2020). To present the results, the model estimates the difference (h_t – h_0) of elevation during the construction of the arc (Fig. 8d).

An outcome of isostatic models is that the surface elevation of the arc rises only after maturing of the buoyant plutonic crust (Fig. 8d). Another relevant point of isostasy is to suggest why the elevation of the arc remains constant or even subsides at an early magmatic stage. Compared to the bulk positive buoyancy of the plutonic crust, the pull-down effect of the root is the most significant when the arc crust is immature (Fig. 8d). Paradoxically, the elevation of the arc rises when the dense root is reaching its maximum thickness. Furthermore, if magmatic thickening is active, root foundering into the mantle causes a bulk uplift of the arc crust (Lee et al., 2015). The lack of a detectable topographic rising, over the Famatinian arc, while the plutonic crust was generated most likely reflects a dearth of massive root foundering during the magmatic constructional stage (section 2.1.). It should be noted that when the Famatinian arc gradually changed from magmatic arc to collision orogeny, the isostatic model should incorporate crustal shortening to magmatic additions (Astini and Dávila, 2004). For this reason, the elevation model for the Famatinian arc between 470 and 465 Ma requires further refinement. To this end, the discussion below addresses the evolution of the Famatinian arc.

3.3. Orogenic model of exhumation

The geology of the Famatinian arc is more intricate than a simple model of an arc shortened, variably uplifted, and eroded during a continent-arc collision (Fig. 9). Despite the intense tectonic contraction, there is some order to the location of plutonic, metasedimentary, and volcano-sedimentary sections (Fig. 9a and b). Tectonic imbrications may be restored using the shear zone pattern and the distribution of Ordovician paleopressures at a regional scale (Figs. 3 and 9). There are few thermochronological data to distinguish the times of synmagmatic regional-aureole metamorphism from that of dynamic metamorphism related to the synorogenic crustal contraction. The available cooling-age data suggest that orogenic convergence was broadly coeval in several different regions of the Famatinian arc (Fig. 9c). Any hypothetical orogenic model should take into account that W-verging attitudes of shear zones are dominant over large regions, whereas E-verging high-strained structures are locally common in the sierras Famatina, Velasco, and San Luis. Both the arrangement and kinematics of shear zones are consistent with a Himalayan-style high-angle convergent scenario (Jamieson et al., 1996; Yin, 2006). The tectonic extrusion of deep crustal sequences was driven by collision of the continental Cuyania microplate (i.e., buoyant indentor) and taken up mostly along W-verging variably inclined shear zones with detached surfaces in the middle and lower crust (Christiansen et al., 2019;

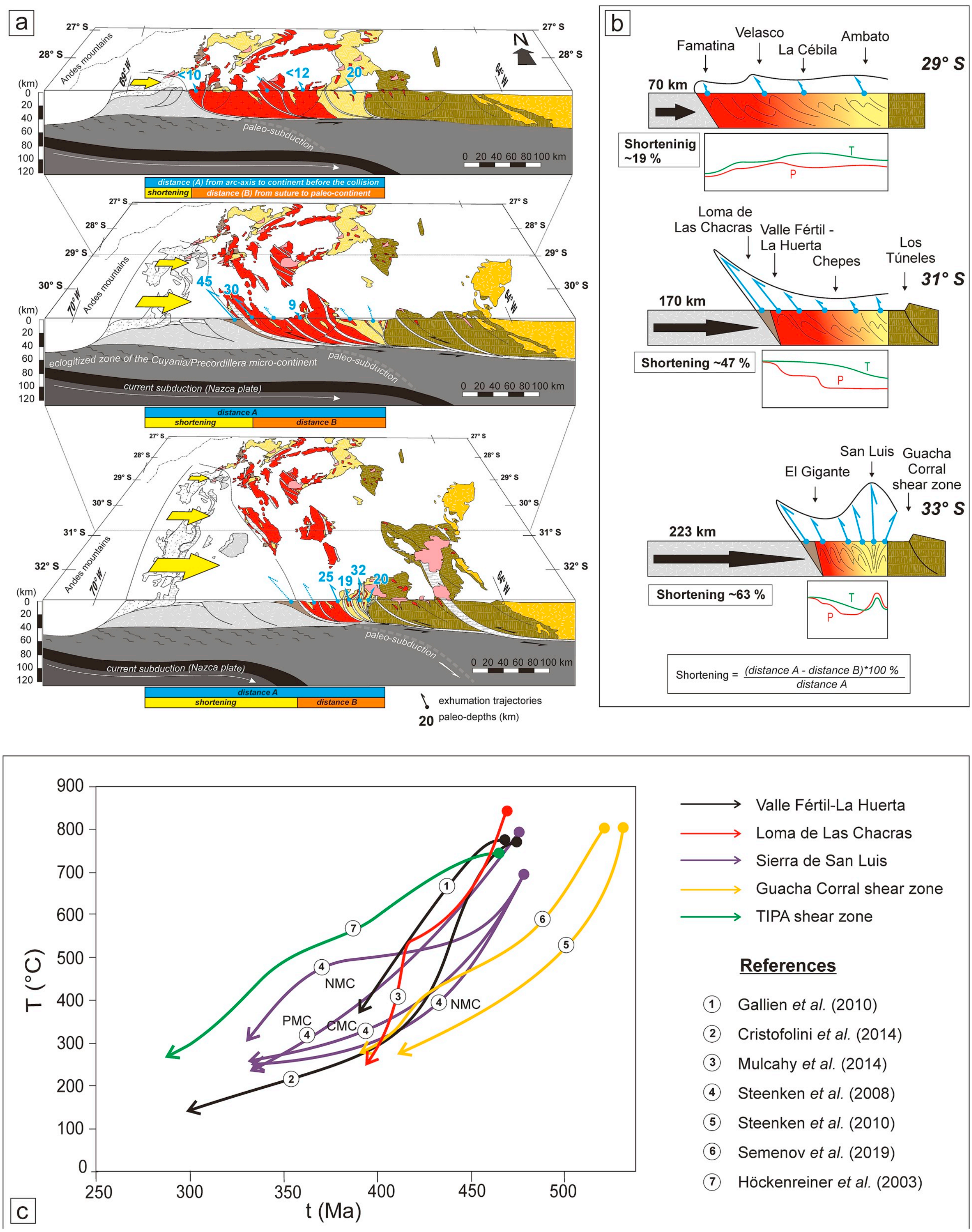

Fig. 9. (a) Diagrammatic 3D models explaining the collisional closure and uplift of the Famatinian arc based on selected literature (Appendix S2). Figure is a reconstructed cross-section of part of the Famatinian arc, in a time frame interpreted to represent the continent-arc collision. **(b)** Schematic material transport within a low-angle convergent scenario. Note that tectonic shortening progressively increased southward and is interpreted to be caused by the indention of the Cuyania/Precordillera microplate. **(c)** Time-temperature paths recorded by isotopic closure temperatures in the retrograde minerals of the Famatinian shear zones documenting that the cooling and uplift evolved over an extended period from the Middle Ordovician to Lower Carboniferous.

Larrovere et al., 2019; and references therein).

A first-order geological feature is spacing among shear zones along the Famatinian arc, the density of shear zones on the present-day surface increases gradually from 28° S to 33° S (Fig. 9a). At the southernmost exposed latitude (33° S), the shear zone system accommodated shortening (≥50 %) through a doubly vergent belt (von Gosen and Prozzi, 1998; Morosini et al., 2014). Within the Sierra de San Luis, the shear zone system records sinistral transpressional with moderate obliquity (Fig. 9b). Stretching lineation in the doubly-vergent belt yields nearly vertical particle paths and explains maximum paleopressures of up to 8 kbar extruded in the core of a km-scale pop-up structure (Ortiz Suárez and Casquet, 2005; Christiansen et al., 2019).

Across the present-day latitude 31° 30' S, a latitudinal reconstruction shows an Ordovician deep-seated plutonic crust thrust over the suture zone formed along the Famatinian–Cuyania/Precordillera collision (Fig. 9a; Cristofolini et al., 2014). The Valle Fértil–La Huerta shear zone, bordering on the eastern flank of the suture zone, detached in the lower crust from the underlying lithosphere and accommodated uplift of up to 30 km of the deep Famatinian plutonic crust (Castro de Machuca et al., 2008; Gallien et al., 2010). The temperature-time history of Valle Fértil–La Huerta shear zone revealed constant cooling during 150 My, even though the cooling rate decreased with time, the interpretation is a record of continuous removal of the overlying crust from the Ordovician to the Early Devonian (Cristofolini et al., 2014). By contrast, the Loma de las Chacras metamorphic complex, which is next to the Valle Fértil shear zone, experienced synorogenic burial during the Paleozoic tectonic contraction (Mulcahy et al., 2014). The small block of Lomas de las Chacras preserves rocks that first were carried at deep depths (> 45 km), then detached off from a subducting channel, and finally uplifted by tectonic extrusion (Casquet et al., 2012; Mulcahy et al., 2014). At the same latitude, the Famatinian batholiths of the sierras Chepes and Las Minas-Ulapes, which are ~100 km eastward from the suture zone, show much less exhumation than plutonic crust located to the west (Fig. 9b).

To the northern latitude 28° 30′ S, the senses of shearing yield subparallel tectonic transport toward the WSW. Maximum synorogenic extrusion centered on backarc crustal sections (Fig. 9a and b). The TIPA shear zone, a crustal-scale shear system, bounds two sections of the plutonic batholith with contrasting uplift (López and Toselli, 1993; Höckenreiner et al., 2003). Both the pattern of paleodepth and the style of deformation suggest a potential décollement (detachment) zone at a depth interval of 20–30 km within the middle crust (Höckenreiner et al., 2003). Most of the tectonic transport is subvertical shear that crossed the ductile-brittle transition at upper-crustal levels. The TIPA zone shows evidence of tectonic shear strain from the Middle Ordovician to Carboniferous times (Höckenreiner et al., 2003). Significantly, thermochronology documents broad synchronicity in the cooling history of the TIPA zone with the other shear zones (Fig. 9c). Within the Famatinian shear zones, mineral retrogression and tectonic cooling initiated during the Middle Ordovician at a cooling rate that first crossed the closure temperatures of $^{40}Ar/^{39}Ar$ in micas (350–300 °C) during the transition from Silurian to Devonian, and then attained the Earth's surface by the Lower Carboniferous (Höckenreiner et al., 2003; Gallien et al., 2010; Castro de Machuca et al., 2008, 2012; Cristofolini et al., 2014; among others).

Contrasting with shear zones developed within the Famatinian arc, the Gaucha Corral and Pachaco shear zones first initiated at the Cambrian, so were already weak crustal-scale belts when Famatinian orogenic convergence expanded in the Pampean orogen (Martino, 2003). The already stabilized Pampean orogen might have acted as a high-strength foreland backstop during the collision-related orogenic stage of the Famatinian arc. Over the Pampean orogen, much of the Famatinian orogenic convergence was taken up along the Guacha Corral shear zone that was active at 470 Ma and so remained until the emplacement of Devonian-Carboniferous post-orogenic batholiths (Martino, 2003; Demartis et al., 2017; Semenov et al., 2019).

4. Geodynamic model for the Famatinian arc

4.1. Pre-conditions for the Famatinian arc on the western Gondwana proto-pacific margin

The Famatinian arc was born outboard of the waning Pampean orogen (Pankhurst and Rapela, 1998). Although it is contentious and not a central focus here, the geodynamic setting of the Pampean orogen is briefly addressed to depict the setting predating the inception of subduction-related Famatinian magmatism. The Pampean orogen initiated at the latest Neoproterozoic during the final assembly of the West Gondwana. At that time, the proto-Andean border of Gondwana began its long history of a destructive margin (Cawood and Buchan, 2007). The subduction-related magmatic stage of the Pampean orogen started at, or early before, 555 ± 5 Ma (Pankhurst and Rapela, 1998; Rapela et al., 2007; Schwartz et al., 2008). At about 535 Ma, a subduction-related magmatic arc entered into a stage of contractional tectonic regime (Schwartz et al., 2008). The accreted metamorphic complexes experienced granulite-facies metamorphism, intracrustal anatexis, and poly-phase ductile deformation over a short time between ~530 and 510 Ma (Guereschi and Martino, 2008; Tibaldi et al., 2019). The contractional tectonic is attributed to a trench-ridge encounter with a trench at the boundary of the Pampean orogen (Schwartz et al., 2008; Tibaldi et al., 2008). Admittedly, the ridge-trench interaction hypothesis is contentious (Rapela et al., 2007) and even less clear is how the tectonic plates reorganized after the spreading ridge subducted beneath the Pampean orogen.

During a late stage of the Pampean orogen, forearc accretionary complexes accreted above the subducting ridge crystallized under high-T metamorphic conditions (Schwartz et al., 2008; Guereschi and Martino, 2008; Tibaldi et al., 2019). Early Cambrian Pampean orogen bounded against an oceanic plate that was on the opposite side of the demised spreading ridge (Perón Orrillo et al., 2019). The amalgamation of the Pampean crystalline sequences to an oceanic plate became the basement of the Middle and Upper Cambrian turbidites. Within this geological context, the San Luis Formation, which record sediment deposited on a deep marine slope and abyssal plain, may contain a unique record of the geological setting where was born the Famatinian arc (Perón Orrillo et al., 2019). It should be noted, however, that Paleozoic crystalline sequences lying to the north of the latitude of 28° S show a slightly different geodynamic evolution at the same time (see Wolfram et al., 2019; and references).

Typical subduction-related magmatism resumed after a period of about 30 My (520–490 Ma) of the magmatic quiescence that followed the Pampean orogen. Accepting that an active ridge subducted beneath the Pampean orogen, the magmatic gap between Pampean and Famatinian systems is compatible with more than one scenery (Fig. 10): either if ridge-trench collision stopped plate converge at *ca.* 515 Ma, a process of subduction zone initiation either spontaneous or induced had to happen in the paleo-Pacific oceanic setting (Izu-Bonin-Mariana style; see Leng and Gurnis, 2015), or if oceanic plate subduction outlasted ridge-trench interaction, subduction-related magmatism would have reestablished when a slab window moved away and a coming oceanic slab began fertilizing the mantle wedge (Chile ridge-trench style; Cande et al., 1987). Nevertheless, solving this problem is beyond the scope of the work.

4.2. Arc growth: petrological process

As documented by field mapping, lithostratigraphic framework, and tectono-thermal evolution, the ancient Famatinian arc is easily separable into a batholithic main arc and a metasedimentary backarc belt (Fig. 1). Another first-order geological feature is the absence of older (Precambrian) basement all over the Famatinian arc, apart from peri-Gondwanan inliers such as the Arequipa Massif (Ramos, 2018). The ancient Famatinian arc growth occurred via subduction driven

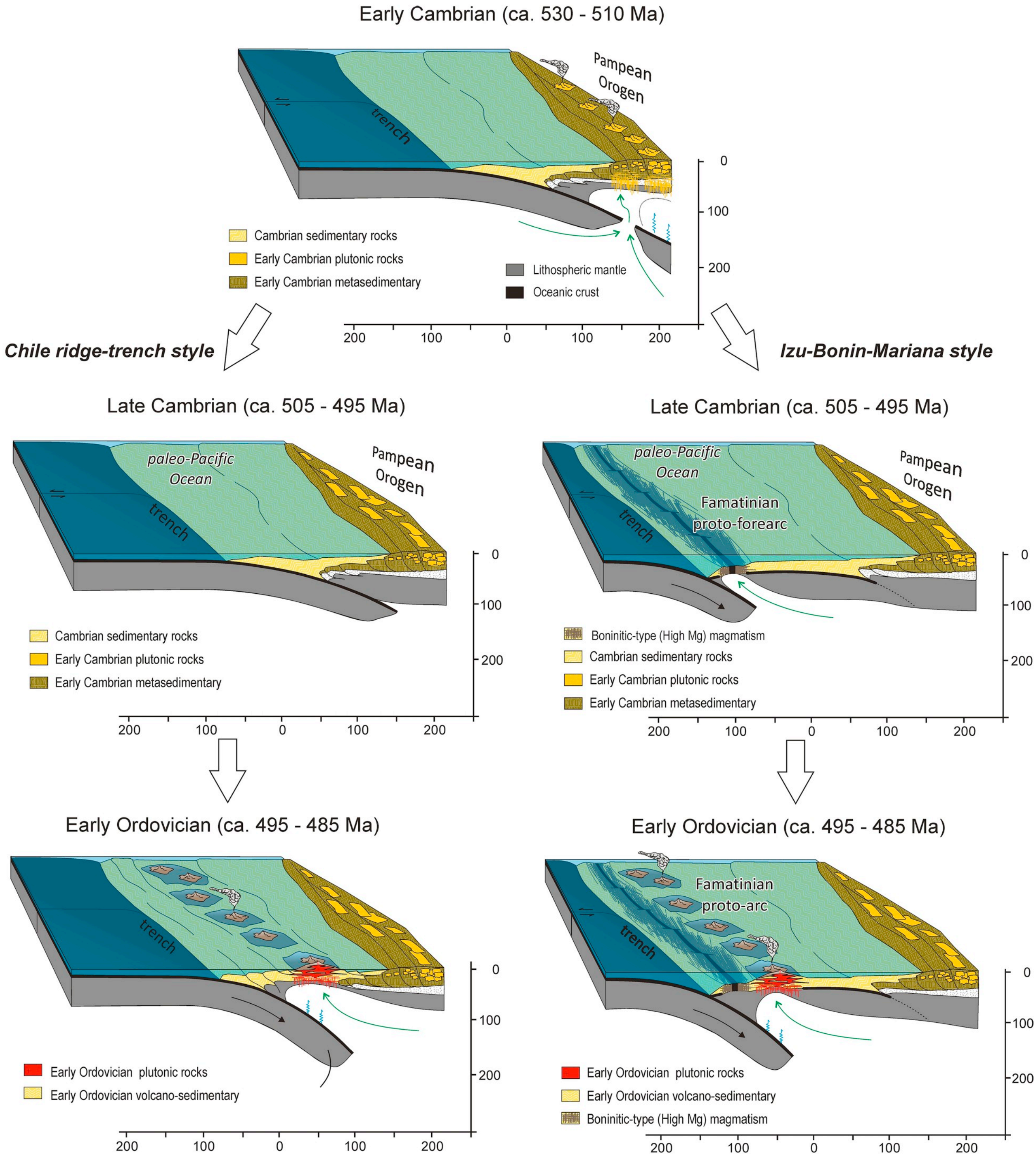

Fig. 10. Diagrammatic models comparing geodynamic sceneries that potentially link the end of the Pampean orogen with a nascent Famatinian arc. On the left side, model is based on knowledge of the Chilean ridge-trench interaction (Cande et al., 1987). An alternative model is an Early Cambrian subduction zone that merged to the Pampean orogen after ridge subduction, and then a nascent Famatinian arc resumed outboard by opening a weakness within an oceanic setting.

magmatism when mantle-melt upwelling emerged and invaded the prearc crust. After 20 My of subduction driven magmatism, the bulk crust of the arc was reconstructed by early Ordovician magmatism. Magmatic construction built up a crustal section lacking a signal of periodicity (Fig. 4). We describe the main steps of evolution and evaluate magma production in the Famatinian arc, but the construction of a crustal section is a spatially and temporally continuous process that left finite observations (Saleeby, 1990).

Both depth-age and depth-chemistry characteristics correspond to that of a transcrustal magmatic system (Bachmann and Bergantz, 2008; Cashman et al., 2017; Putirka, 2017). Yet, a singular aspect is a magmatic system that has not a well-defined lithological stratification across crustal paleodepths and along the paleo-arc axis (Figs. 4 and 5). The deep-seated plutonic section of the Sierra de Valle Fértil-La Huerta enables inferring how is the unexposed crust over the shallow batholiths from the sierras Famatina, Velasco, Chepes and Las Minas-Ulapes (Figs. 1 and 3). The generation of the Famatinian arc crustal section is deconstructed using a field-based 3D perspective. The plutonic construction was bottom up and driven by emplacement of mafic melts into and onto a progressively heated and magmatically evolving mantle-crust transition (Otamendi et al., 2012; Walker et al., 2015). Upon leaving behind their mantle sources, hydrous mafic magmas either stalled in the low crust or ascended throughout the middle crust (Saal, 1993; Saavedra et al., 1998; Alasino et al., 2016; Camilletti et al., 2020). Mafic magmatism was not only the origin of synmagmatic mafic dikes and microgranular mafic inclusions that are widely dispersed over the middle and upper plutonic crust but also fed basaltic lava flows and microgabbroic sills emplaced into the volcano-sedimentary sequences (Fig. 2; see Mannheim, 1993). Continued mantle-derived magmatic addition into the mantle-crust transition activates deep-seated layers of tonalitic mushes, which then mature to supply the quartzo-feldspathic middle plutonic crust (Hildreth and Moorbath, 1988; Saleeby, 1990; Annen and Sparks, 2002). As Jagoutz (2010) and Walker et al. (2015) showed, incubation and generation of intermediate melts inside a MASH-like low crustal zone has a complexity that is not captured by simple mechanical separation of early crystallizing minerals and melt that yields magmatic differentiation.

On top of the lower mafic crust, a km-thick tonalitic-dominated plutonic section is a crystallized product of plutonic levels fed by derivate melt that left behind a mafic cumulate sequence (Otamendi et al., 2012; Tibaldi et al., 2013; Walker et al., 2015; Camilletti et al., 2020). When the middle crust had grown up into a tonalitic-dominated magmatic sequence, it became the framework that expanding upward constructed the upper silicic zone (Bachmann and Bergantz, 2008). The constant and massive influx of mafic magmatism caused the melting of pre-arc crust and enhanced hybridization between mantle-sourced and continentally-derived materials. Overlying the tonalitic plutonic crust, granodiorites, and granites that made up the silicic upper crust are derivative products of tonalitic mushy magmas that evolved through plagioclase- and amphibole-dominated fractionation, and assimilated metasedimentary rocks with their anatectic leucogranitic component (Otamendi et al., 2012). Silicic plutonic and volcanic sequences dominating the upper crust are both fractionated and well-mixed lithological products. Three magmatic sources fed the shallow plutonic crust and the volcanic system, these were: 1) mafic melts ascending from the lower mafic crust, 2) intermediate and silicic magmas (mushes) rising from the middle crust, and 3) intra-crustal rhyolitic melts from the middle and upper crust (Mannheim, 1993; Cisterna and Coira, 2014; Alasino et al., 2016; Armas et al., 2018).

4.3. Arc growth: magmatic tempo

To estimate the long-term magmatic fluxes, we use the along-arc-strike type segment from Valle Fértil to the northern Sierra de Famatina (Fig. 1; see Tibaldi et al., 2013). Within this Famatinian arc segment, most of the plutonic rocks are compositionally well characterized (Fig. 5), and outside the shear zones, they preserve the magmatic structure (Fig. 6). The approach to reckon the magmatic tempo is based on field observations, which permit reconstructing a 3D arc crustal section dominated by plutonic rocks, and uses the dataset of available U-Pb zircon crystallization ages (Fig. 4). For these reasons, the estimate of magmatic addition rates is just a first-order approximation, but, as a single magmatic cycle, provides a useful comparison to episodic magmatic tempo elsewhere.

The batholithic-scale plutonic and volcanic crustal column is reconstructed up to paleodepth of about 30 km and timed to have grown during 17 My (485–468 Ma) at volumetric magmatic fluxes of about 1.76 km^3/My per km^2 of active arc surface. Although, rather than being time-averaged magmatic fluxes from the mantle to the crust, the result is a frozen record of construction and preservation of an ancient crustal cross-section. One relevant question is whether all the plutonic/volcanic masses come from the mantle or just a part of it. The answer is simple, the Famatinian arc consists of less than about 20 vol percent of the original pre-arc crust over the main batholitic belt (Fig. 1). It implies that a large mass of the original host rocks has been reconstructed into the plutonic/volcanic rocks across the entire sequence of the exposed paleodepths (Otamendi et al., 2012; Tibaldi et al., 2013). Another aspect complicating the interpretation is how much mantle-sourced magmatic fluxes made cumulate which is no longer traceable. A minimum mass fraction of generated cumulate broadly equals the exposed mass of intermediate and silicic plutonic rocks less the pre-arc crustal mass cannibalized into plutonic rocks (Camilletti et al., 2020). A question immediately arises, where are the cumulate rocks that complement to plutonic rocks more evolved than gabbros in the Famatinian arc. A simple answer is that tens of kilometers of cogenetic cumulates are lost. However, it is still open the question of whether dense cumulate roots were either delaminated over the magmatic stage or tectonically removed during the collisional-related uplift, or a combination of both processes.

Last but not least is the problem of preservation. The collisional closure of the Famatinian arc presents a crucial challenge to calculate the volume addition rate per arc length ($km^3km^{-1}My^{-1}$). It is unclear to what extent the main arc is shortened (section 3.3; see Christiansen et al., 2019). To the south of latitude 27° S, the Famatinian arc is both contracted and differentially uplifted. At the latitude 29° S, the preserved across-arc section is 140 km wide over the plutonic Ordovician crust enabling to estimate a minimum magma production rate of about 250 $km^3km^{-1}My^{-1}$. Since the estimate of magma production rate utilizes the full-time span in the geochronological dataset, the result yields a lower value than that of Ducea et al. (2017). Nevertheless, with all the uncertainties in mind, it remains true that the Famatinian arc growth is entirely a high-magma-production period.

4.4. Continent-arc collisional evolution

The Famatinian arc developed near the West Gondwana margin, on the western side of a rather narrow backarc basin that never reached the stage of an oceanic basin (Mannheim, 1993). During most of the Lower - Middle Ordovician, a voluminous arc plutonic crust developed while the stress regime in the overriding plate controlled the opening of intra-arc and backarc basins (Fig. 11a). Sometime in the Middle Ordovician, the last remnants of an ocean in the Iapetus (paleo-Pacific) realm began closing with the entry of the Cuyania/Precordillera continental plate in the subduction zone (Astini and Dávila, 2004; Benedetto, 2004). The early convergent history of the Famatinian arc is signaled by folding and thrusting deformation of the volcano-sedimentary successions (Astini and Dávila, 2004). An angular unconformity marks the onset of convergent tectonic coeval with the sedimentation of the Middle Ordovician strata (Astini and Dávila, 2004). Subduction-related magmatism outlived tectonic contraction over a few millions of years, but subduction-related magmatism gradually waned and stopped at about 465 Ma (Ducea et al., 2010; Rapela et al., 2018). Synchronously, voluminous flysch-like sediments (Gualcamayo Formation) shed away from the incipient collisional zone filled the foreland in the subducting plate (Fig. 11b; Astini, 1998; Benedetto, 2004).

The transition from subduction to collision at *ca.* 470 Ma took a few million years before maturing into a hard continent-arc collision (Benedetto, 2004). At that point, lithosphere-scale convergence caused accretion of plutonic and metamorphic crystalline arc crust while the detached underlying lithosphere subducted (Astini and Dávila, 2004). The final welding between the Cuyania/Precordillera microplate and the closing Famatinian arc occurred at the Middle - Upper Ordovician (Darriwilian - Sandbian) and associated with a prolonged stage of Molasse-like clastic wedge shed onto the downgoing continental plate (Astini, 2003). It initiated the development of substantial uplift (mountain-building process) within a hard collision in which both plates were strongly deformed (Astini and Dávila, 2004; Mulcahy et al., 2014; Cristofolini et al., 2014). At some point of the continent-arc collision, the overriding Famatinian arc became mechanically decoupled from the complementary lithospheric mantle, the entire main arc and backarc crystalline sequences experienced rapid uplift rates (Fig. 11c).

The continental Cuyania microplate with an irregular geometry towards the direction of indentation shaped the deformation style over

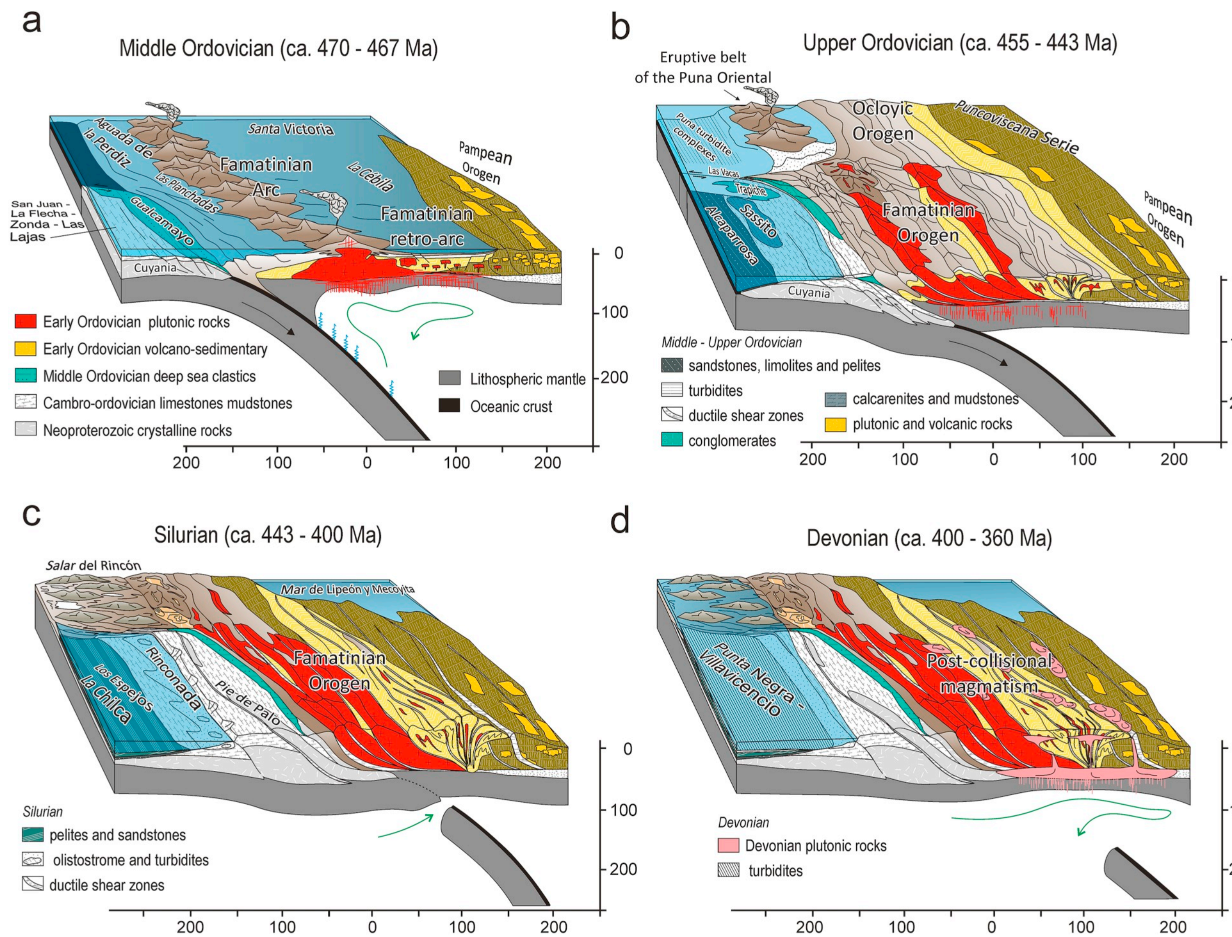

Fig. 11. Schematic tectonic model for the continent-arc collision orogeny modified from Cristofolini et al. (2014) and Christiansen et al. (2019). Main steps are **(a)** the closure of an oceanic basin led to the onset of subduction of a continental microplate (Cuyania/Precodillera terrane). Interaction of two buoyant plates slowed subduction along a segment of the overriding Famatinian arc. **(b)** In the Upper Ordovician, the Cuyania/Precordillera microplate advanced into the Famatinian arc locking the subduction zone and contracting the overriding plate. **(c)** During the Silurian, a mature continent-arc collisional orogen forced unroofing of the Famatinian batholithic crust, stacked backarc metasedimentary succession, juxtaposed deep onto shallow Famatinian sequences, and further uplifted the Cambrian Pampean orogen. **(d)** After more than 70 My of orogenic growth, the Cuyania-Famatinian orogen began collapsing. Positive topography endured until the Pennsylvanian epoch when the first post-orogenic sediments filled continental basins within the eroded Famatinian basement (not shown).

the overriding Famatinian orogen (e.g., Astini and Dávila, 2004; von Gosen and Prozzi, 2005; Christiansen et al., 2019). Within a vanished Famatinian arc, the trajectories of exhumation chiefly reflect the impact of the tectonic indenter on driving contraction and uplift (Fig. 9a–b). At a mature stage, collision orogeny broadened the hinterland, expanded into the foreland, and further uplifted the Cambrian Pampean orogen (Martino, 1993; Demartis et al., 2017; Semenov et al., 2019). Within this context, continued lithospheric convergence within the central part of the Famatinian arc by bivergent (retro- and pro-wedge) high-angle thrusting drove of crustal shortening in the core of the orogenic hinterland (Morosini et al., 2014). Overall the overriding orogenic system records protracted shearing over a long period from the Middle Ordovician (pre-Hirnantian) to the Silurian (Ludlow - Ludfordian), with a local reworking of shear zone reaching the Lower Devonian (Pragian). By the late Devonian and early Carboniferous time, the Famatinian arc orogenic crust should have been extended and spread by orogenic collapse (Fig. 11d). The temperature in the lower part of a stretching crust increased enough to melt it and produces post-orogenic magmatism (Morosini et al., 2017). Positive topography endured even longer to the late Carboniferous when continental sediments filled shallow sedimentary basins.

5. Further implications and future challenges

The geodynamic model is adequate to elucidate the observed data and to make realistic inferences on the nature of the Famatinian arc. No claim is made for the model beyond these facts. Today, several research lines are reasonably well developed, among which are the studies producing stratigraphic, paleontological, geochronological, petrological, and geochemical (elemental and isotopic) data. Nonetheless, some questions remain open. A research line that might provide better constraints on the orogenic model is the study of shear zones combining structural geology and thermochronology (Semenov et al., 2019; Larrovere et al., 2019). Another approach with a future is high-precision geochronology that helps to tightly bracketed magmatic tempos (Ducea et al., 2017). Finally, more data of isotopes in zircons might open the plutonic archive to ponder whether magmas formed by the digesting of metasedimentary materials into evolving mantle-like magmas or by remelting ancient continental crust (Rapela et al., 2018).

Here, we discuss two issues that require further data. One is surveying the infant stages of the Famatinian arc. Most of what is known about subduction initiation comes from the active western Pacific subduction zones (Stern and Bloomer, 1992; Ishizuka et al., 2014; among others). Some aspects of this knowledge are important for understanding the Famatinian arc. First, it begins with the conversion of a subduction-transform edge propagator plate-scale system into a proto-trench system

(Stern and Bloomer, 1992; Toth and Gurnis, 1998). Second, over a nascent subduction zone, the sinking lithosphere causes trench rollback and allows the entrance of asthenospheric upwelled melt into the space that the subducting plate liberates (Stern and Bloomer, 1992). Third, the lithosphere, including a plutonic-volcanic thin crust and a refractory mantle, becomes the basement for a coming magmatic arc (Ishizuka et al., 2014; Leng and Gurnis, 2015). With outstanding geological insights, Mannheim (1993) showed that the nascent Famatinian arc stage was a rifted-arc stage, and also suggested that the Famatinian arc retreated to a position outboard during its inception. In this regard, the Negro Peinado angular unconformity in the Sierra de Famatina may be a unique trait of developing east-dipping subduction along a nascent edge that was located westward. Up to now, there is no vestige of crustal remnants formed during initial subduction. Over the segment of interest, there are few prospects to find infant arc fragments in the Famatinian forearc as the continent-arc collision orogeny removed the forearc and juxtaposed the plutonic Famatinian crust onto the tectonic suture (Cristofolini et al., 2014). Within the region dominated by main arc batholiths, the infant arc foundational crust has been reworked in generating plutonic rocks. A rare expectation is surveying metamorphic complexes that evolved on the backarc side and preserved fragments of nascent arc crust. The Nogoli metamorphic complex in the Sierra de San Luis is a plausible candidate (González et al., 2009). An argument line to develop is that the proto-Famatinian crust was overwhelmingly dominated by the lithosphere formed during the Famatinian infant arc magmatism (Fig. 10). This idea might explain two problems of the Famatinian arc. These are the absence of pre-arc crust and the predominance of subduction-related rocks with continental isotopic signatures. The absence of pre-arc crust is due to the thin infant crust was rapidly assimilated in the arc construction of the plutonic batholiths. The Famatinian lithosphere may have acquired its continental isotopic signature during the subduction zone inception. A young slab sinking into the upper mantle and carrying craton-derived sediments might have released the metasomatic agents that serpentinized the sub-Moho mantle and metasomatized the prearc crust (Stern and Bloomer, 1992).

The other priority research is better assessing the impact of Famatinian arc evolution on the responses of the Andean foreland to ongoing tectonic forces. At a very fundamental level, the goal of the geoscientist community is to keep on refining an integrated explanation between synorogenic mountain-building expressions and pre-orogenic paleogeographic influences, for which the Sierras Pampeanas over the Pampean flat-slab segment is a challenging natural example. The structural styles of the Andean foreland deformation vary along strike with a marked change at 26–27 °S. At this latitude, thin-skinned and thick-skinned fold-and-thrust belts characterizing the Cordillera Oriental and Sierras Subandinas become basement-cored uplifts in the Sierras Pampeanas (Jordan and Allmendinger, 1986; Allmendinger and Gubbels, 1996; Kley et al., 1999; Ramos et al., 2002). The structural segmentation of the foreland implies along-strike variations in 1) the dip angle of the subducting Nazca plate, 2) both the timing and amount of shortening of the overriding Sudamericana plate, and 3) the rheological stratification of the lithosphere in the foreland (Allmendinger and Gubbels, 1996; Kley et al., 1999). While the first two controls are inter-related and determined by Cenozoic plate tectonic, the paleogeographic evolution of foreland segments is the third controlling factor. By middle Neogene, when the Nazca plate began flattening, the Sierras Pampeanas were plains with thin sedimentary covers overlying shallow crystalline basements (Allmendinger and Gubbels, 1996; Ramos et al., 2002). Under Cenozoic tectonic convergence, Paleozoic shear zones were reactivated to NW-SE-striking brittle-ductile faults uplifting crystalline ranges over the Sierras Pampeanas (Figs. 6 and 9). The tectonic-morphologic expression is related to crustal weakness inherited from the Paleozoic history. The Sierras Pampeanas is an Andean exhumed basement-cored broken foreland that originally formed in the hinterland of a Paleozoic collisional orogen. Yet interestingly, the décollement depths accommodating crustal shortening in the Central Andes coincide with the paleodepth inferred for the Famatinian tectonic uplift (Snyder et al., 1990).

Acknowledgment

We thank an anonymous reviewer for a thoughtful and helpful review of the manuscript. The comments and recommendations from Editor Prof. Andrés Folguera assisted us in significantly improving the manuscript. We express our gratitude to numerous people for discussions, support with fieldwork and assistance with analytical work over the years, including Matías Barzola, George Bergantz, Fernando Cañas, Julien Cornet, Alejandro Demichelis, Mihai Ducea, Facundo Escribano, Roberto Martino, Ariel Ortiz Suárez, Jesús de la Rosa, and Graciela Vujovich. We are deeply indebted to Zack McIntire, a Ph.D. candidate at the University of Washington, who reviewed the writing style. For 15 years the research was supported by CONICET, Mincyt, Foncyt, and Secyt-UNRC, Argentina. This review has cited as many important papers as possible, a long list of references so far, but as always with reviews, due credit involves to only a short part of the community that has contributed original and transcendental research; we apologize in advance for missing important studies.

Appendix A. Supplementary data

Supplementary data to this article can be found online at https://doi.org/10.1016/j.jsames.2020.102558.

References

Aceñolaza, F.G., Toselli, A.J., 1977. Observaciones geológicas y paleontológicas sobre el Ordovícico de la zona de Chaschuil, Provincia de Catamarca. Acta Geol. Lilloana 14, 55–81.

Alasino, P., Casquet, C., Larrovere, M., Pankhurst, R., Galindo, C., Dahlquist, J., Rapela, C., 2014. The evolution of a mid–crustal thermal aureole at Cerro Toro, Sierra de Famatina, NW Argentina. Lithos 190, 154–172.

Alasino, P., Casquet, C., Pankhurst, R., Rapela, C., Dahlquist, J., Galindo, C., Baldo, E., 2016. Mafic rocks of the Ordovician Famatinian magmatic arc (NW Argentina), new insights into the mantle contribution. Geol. Soc. Am. Bull. 128, 1105–1120.

Allmendinger, R., Gubbels, T., 1996. Pure and simple shear plateau uplift, Altiplano-Puna, Argentina and Bolivia. Tectonophysics 259, 1–13.

Annen, C., Sparks, R.S., 2002. Effects of repetitive emplacement of basaltic intrusions on thermal evolution and melt generation in the crust. Earth Planet Sci. Lett. 203, 937–955.

Arculus, R.J., 2003. Use and abuse of the terms calcalkaline and calcalkalic. J. Petrol. 44, 929–935.

Armas, P., Cristofolini, E., Otamendi, J., Tibaldi, A., Barzola, M., 2016. Caracterización de las facies volcano–sedimentarias de la formación Chuschín, sector sur–Occidental del sistema de Famatina, provincia de La Rioja. Rev. Asoc. Geol. Argent. 73, 78–92.

Armas, P., Cristofolini, E.A., Otamendi, J.E., Tibaldi, A.M., Barzola, M.G., Camilletti, G.C., 2018. Geochronology and facies analysis of subaqueous volcanism of Lower Ordovician, Famatinian arc, Argentina. J. S. Am. Earth Sci. 84, 255–265.

Astini, R., 1998. El Ordovícico de la región central del Famatina (provincia de La Rioja, Argentina), aspectos estratigráficos, geológicos y geotectónicos. Rev. Asoc. Geol. Argent. 53, 445–460.

Astini, R., 2003. The Ordovician proto–Andean basins. In: Benedetto, J.L. (Ed.), Ordovician fossils of Argentina. Secretaría de Ciencias y Tecnología. Universidad Nacional de Córdoba, Córdoba, pp. 1–74.

Astini, R., Benedetto, J.L., 1996. Paleoenviromental features and basin evolution of a complex volcanic– arc region in the Pre–Andean western Gondwana, the Famatina belt. In: 3° International Symposium on Andean Geodynamic, pp. 755–758.

Astini, R., Dávila, F., 2004. Ordovician back arc foreland and Ocloyic thrust belt development on the western Gondwana margin as a response to Precordillera terrane accretion. Tectonics 23, TC4008.

Bachmann, O., Bergantz, G.W., 2008. Rhyolites and their source mushes across tectonic settings. J. Petrol. 49, 2277–2285.

Bachmann, O., Huber, C., 2018. The inner workings of crustal distillation columns; the physical mechanisms and rates controlling phase separation in silicic magma reservoirs. J. Petrol. 60, 3–18.

Benedetto, J.L., 1994. Braquiópodos ordovícicos (Arenigiano) de la Formación Suri en la región del río Chaschuil, Sistema del Famatina, Argentina. Ameghiniana 31, 221–238.

Benedetto, J.L., 2004. The allochthony of the Argentine Precordillera ten years later (1993–2003), a new paleobiogeographic test of the microcontinental model. Gondwana Res. 7, 1027–1039.

Bouilhol, P., Schmidt, M.W., Burg, J.P., 2015. Magma transfer and evolution in channels within the arc crust: the pyroxenitic feeder pipes of Sapat (Kohistan, Pakistan). J. Petrol. 56, 1309–1342.

Bowen, N.L., Schairer, J.F., 1935. The system MgO-FeO-SiO_2. Am. J. Sci. 170, 151–217.

Büttner, S.H., Glodny, J., Lucassen, F., Wemmer, K., Erdmann, S., Handler, R., Franz, G., 2005. Ordovician metamorphism and plutonism in the Sierra de Quilmes metamorphic complex, implications for the tectonic setting of the northern Sierras Pampeanas (NW Argentina). Lithos 83, 143–181.

Camilletti, G., Otamendi, J., Tibaldi, A., Cristofolini, E., Leisen, M., Romero, R., Armas, P., Barzola, 2020. Geology, petrology, and age of Sierras Valle Fértil - La Huerta batholith: implications for the construction of arc crustal magmatic columns. J. S. Am. Earth Sci. 97, 102423.

Cande, S., Leslie, R.B., Parra, J.C., Hobart, M., 1987. Interaction between the Chile Ridge and Chile Trench: geophysical and geothermal evidence. J. Geophys. Res.: Solid Earth 92, 495–520.

Candiani, J.C., Astini, R., Dávila, F., Collo, G., Ezpeleta, M., Alasino, P., Dahlquist, J., Carrizo, R., 2011. Hojas Geológicas 2969–18 Famatina Y 2969–24, Sañogasta, 1,100.000. Boletín 379. Instituto de Geología y Recursos Minerales, Buenos Aires.

Cao, W., Paterson, S., 2016. A mass balance and isostasy model: exploring the interplay between magmatism, deformation and surface erosion in continental arcs using central Sierra Nevada as a case study. G-cubed 17, 2194–2212.

Carugno Duran, A., Ortiz Suárez, A., 2012. Las metamorfitas de baja presión en la sierra de Sococscora, San Luis, y sus implicancias regionales. Rev. Asoc. Geol. Argent. 69, 187–194.

Cashman, K.V., Sparks, R.S., Blundy, J.D., 2017. Vertically extensive and unstable magmatic systems, a unified view of igneous processes. Science 355 eaag3055.

Casquet, C., Rapela, C., Pankhurst, R., Baldo, E., Galindo, C., Fanning, C., Dahlquist, J., 2012. Fast sediment underplating and essentially coeval juvenile magmatism in the Ordovician margin of Gondwana, Western Sierras Pampeanas, Argentina. Gondwana Res. 22, 664–673.

Castro de Machuca, B., Arancibia, G., Morata, D., Belmar, M., Previley, L., Pontoriero, S., 2008. P-T-t evolution of an Early Silurian medium-grade shear zone on the west side of the Famatinian magmatic arc, Argentina: implications for the assembly of the Western Gondwana margin. Gondwana Res. 13, 216–226.

Castro de Machuca, B., Delpino, S., Previley, L., Mogessie, A., Bjerg, E., 2012. Tectonometamorphic evolution of a high- to medium-grade ductile deformed metagabbro/metadiorite from the Arenosa Creek shear zone, western sierras Pampeanas, Argentina. J. Struct. Geol. 42, 261–278.

Cawood, P.A., Buchan, C., 2007. Linking accretionary orogenesis with supercontinent assembly. Earth Sci. Rev. 82, 217–256.

Chin, E.J., Shimizu, K., Bybee, G.M., Erdman, M.E., 2018. On the development of the calc-alkaline and tholeiitic magma series: a deep crustal cumulate perspective. Earth Planet Sci. Lett. 482, 277–287.

Christiansen, R., Morosini, A., Enriquez, E., Muñoz, B., Klinger, F., Martinez, M., Ortiz Suárez, A., Kostadinoff, J., 2019. 3D litho-constrained inversion model of southern Sierra Grande de San Luis: new insights into the Famatinian tectonic setting. Tectonophysics 756, 1–24.

Cisterna, C.E., 1992. Granitoides Paleozoicos de la Sierra de Narváez, Sistema de Famatina, Argentina, Hibridización de Magmas en un Margen Continental Activo. Estud. Geol. 48, 229–235.

Cisterna, C.E., Coira, B., 2014. Subaqueous eruption–fed mass–flow deposits, records of the Ordovician arc volcanism in the Northern Famatina Belt, Northwestern Argentina. J. S. Am. Earth Sci. 49, 73–84.

Conci, I.D., Dávila, F.M., Astini, R.A., Martino, R.D., 2001. La faja de deformación de Chuschín (29°17' S), sierra de Famatina, provincia de La Rioja, Argentina. Asociación Geológica Argentina, Serie D. Publicación Especial 5, 117.

Cristofolini, E., Otamendi, J., Walker Jr., B., Tibaldi, A., Armas, P., Bergantz, G., Martino, R., 2014. A Middle Paleozoic shear zone in the Sierra de Valle Fértil, Argentina, Records of a continent–arc collision in the Famatinian margin of Gondwana. J. S. Am. Earth Sci. 56, 170–185.

Dahlquist, J.A., Pankhurst, R., Rapela, C.W., Galindo, C., Alasino, P., Fanning, C., Baldo, E.G., 2008. New SHRIMP U–Pb data from the Famatina complex, constraining early–mid ordovician famatinian magmatism in the Sierras Pampeanas, Argentina. Geol. Acta 6, 319–333.

Dahlquist, J.A., Rapela, C.W., Baldo, E.G., 2005. Petrogenesis of cordierite-bearing S-type granitoids in Sierra de Chepes, Famatinian orogen, Argentina. J. S. Am. Earth Sci. 20, 231–251.

Davies, J.H., Stevenson, D.J., 1992. Physical model of source region of subduction zone volcanics. J. Geophys. Res., Solid Earth 97, 2037–2070.

DeBari, S., 1994. Petrogenesis of the Fiambalá gabbroic intrusion, northwestern Argentina, a deep crustal syntectonic pluton in a continental magmatic arc. J. Petrol. 35, 679–713.

DeBari, S., 1997. Evolution of magmas in continental and oceanic arcs, the role of the lower crust. Can. Mineral. 35, 501–519.

DeBari, S., Greene, A., 2011. Vertical stratification of composition, density, and inferred magmatic processes in exposed arc crustal sections. In: Arc-continent Collision. Springer, pp. 121–144.

Demartis, M., Jung, S., Berndt, J., Aragón, E., Sato, A.M., Radice, S., Maffini, M., Coniglio, J., Pinotti, L., D'eramo, F., Agulleiro, L., 2017. Famatinian inner arc, Petrographical observations and geochronological constraints on pegmatites and leucogranites of the Comechingones pegmatitic field (Sierras de Córdoba, Argentina). J. S. Am. Earth Sci. 79, 239–253.

Ducea, M., 2001. The California arc: thick granitic batholiths, eclogitic residues, lithospheric-scale thrusting, and magmatic flare-ups. GSA Today (Geol. Soc. Am.) 11, 4–10.

Ducea, M., Bergantz, G., Crowley, J., Otamendi, J., 2017. Ultrafast magmatic buildup and diversification to produce continental crust during subduction. Geology 45, 235–238.

Ducea, M., Otamendi, J., Bergantz, G., Stair, K., Valencia, V., Gehrels, G., 2010. Timing constraints on building an intermediate plutonic arc crustal section, U–Pb zircon geochronology of the Sierra Valle Fértil, Famatinian Arc, Argentina. Tectonics 29, TC4002.

England, P.C., Katz, R.F., 2010. Melting above the anhydrous solidus controls the location of volcanic arcs. Nature 467, 700.

Esteban, S., 1993. Litofacies de plataforma en la Formación Volcancito (Tremadociano) flanco oriental de la Sierra de Famatina, La Rioja. 12° Congreso Geológico Argentino Acta 1, 116–120.

Esteban, S.B., 2002. The Early Ordovician in the Sistema de Famatina: stratigraphic and geotectonic framework. INSUGEO, Serie Correlación Geológica 16, 7–16.

Finch, M.A., Weinberg, R.F., Hasalová, P., Becchio, R., Fuentes, M.G., Kennedy, A., 2017. Tectono–metamorphic evolution of a convergent back–arc, the Famatinian orogen, Sierra de Quilmes, Sierras Pampeanas, NW Argentina. Geol. Soc. Am. Bull. 129, 1602–1621.

Gallien, F., Mogessie, A., Bjerg, E., Delpino, S., de Machuca, B.C., Thöni, M., Klötzli, U., 2010. Timing and rate of granulite facies metamorphism and cooling from multi-mineral chronology on migmatitic gneisses, Sierras de La Huerta and Valle Fértil, NW Argentina. Lithos 114, 229–252.

González, P., Sato, A., Llambías, E., Petronilho, L., 2009. Petrology and geochemistry of the banded iron formation in the eastern sierras Pampeanas of san Luis (Argentina): implications for the evolution of the Nogolí metamorphic complex. J. S. Am. Earth Sci. 28, 89–112.

Grosse, P., Bellos, L.I., Camilo, R., Larrovere, M.A., Rossi, J.N., Toselli, A.J., 2011. Across–arc variation of the Famatinian magmatic arc (NW Argentina) exemplified by I–, S–and transitional I/S–type Early Ordovician granitoids of the Sierra de Velasco. J. S. Am. Earth Sci. 32, 110–126.

Guereschi, A., Martino, R., 2008. Field and textural evidence of two migmatization events in the Sierras de Córdoba, Argentina. Gondwana Res. 13, 176–188.

Hauzenberger, C.A., Mogessie, A., Hoinkes, G., Felfernig, A., Bjerg, E.A., Kostadinoff, J., Delpino, S., Dimieri, L., 2001. Metamorphic evolution of the Sierras de San Luis, Argentina: granulite facies metamorphism related to mafic intrusions. Mineral. Petrol. 71, 95–126.

Hildreth, W., Moorbath, S., 1988. Crustal contributions to arc magmatism in the Andes of central Chile. Contrib. Mineral. Petrol. 98, 455–489.

Höckenreiner, M., Söllner, F., Miller, H., 2003. Dating the TIPA shear zone: an Early Devonian terrane boundary between the Famatinian and Pampean systems (NW Argentina). J. S. Am. Earth Sci. 16, 45–66.

Ishizuka, O., Tani, K., Reagan, M.K., 2014. Izu–Bonin–Mariana fore-arc crust as a modern ophiolite analogue. Elements10 115–120.

Jagoutz, O., 2010. Construction of the granitoid crust of an island arc. Part II, a quantitative petrogenetic model. Contrib. Mineral. Petrol. 160, 359–381.

Jagoutz, O., 2014. Arc crustal differentiation mechanisms. Earth Planet Sci. Lett. 396, 267–277.

Jagoutz, O., Klein, B., 2018. On the importance of crystallization-differentiation for the generation of SiO2-rich melts and the compositional build-up of arc (and continental) crust. Am. J. Sci. 318, 29–63.

Jagoutz, O., Müntener, O., Schmidt, M.W., Burg, J.P., 2011. The roles of flux-and decompression melting and their respective fractionation lines for continental crust formation: evidence from the Kohistan arc. Earth Planet Sci. Lett. 303, 25–36.

Jamieson, R.A., Beaumont, C., Hamilton, J., Fullsack, P., 1996. Tectonic assembly of inverted metamorphic sequences. Geology 24, 839–842.

Jones, D.W., Katz, R.F., Tian, M., Rudge, J.F., 2018. Thermal impact of magmatism in subduction zones. Earth Planet Sci. Lett. 481, 73–79.

Jordan, T.E., Allmendinger, R.W., 1986. The Sierras Pampeanas of Argentina, a modern analogue of Rocky Mountain foreland deformation. Am. J. Sci. 286, 737–764.

Kelemen, P.B., Hanghøj, K., Greene, A.R., 2003b. One view of the geochemistry of subduction-related magmatic arcs, with an emphasis on primitive andesite and lower crust. Treatise Geochem. 3, 659.

Kelemen, P.B., Rilling, J.L., Parmentier, E.M., Mehl, L., Hacker, B.R., 2003a. Thermal structure due to solid-state flow in the mantle wedge beneath arcs. Geophys. Monograph-Am. Geophys. Union 138, 293–311.

Kelley, K.A., Cottrell, E., 2009. Water and the oxidation state of subduction zone magmas. Science 325, 605–607.

Keppie, J.D., Ramos, V.A., 1999. Odyssey of Terranes in the Lapetus and Rheic Oceans During the Paleozoic 336. pp. 267–276 Laurentia-Gondwana connections before Pangea.

Kley, J., Monaldi, C., Salfity, J., 1999. Along-strike segmentation of the Andean foreland: causes and consequences. Tectonophysics 301, 75–94.

Larrovere, M.A., de los Hoyos, C., Toselli, A., Rossi, J., Basei, M., Beldar, M., 2011. High T/P evolution and metamorphic ages of the migmatitic basement of Northern Sierras Pampeanas, Argentina, characterization of a mid–crustal segment of the Famatinian belt. J. S. Am. Earth Sci. 31, 279–297.

Larrovere, M.A., de los Hoyos, C., Willner, A., Verdecchia, S., Baldo, E., Casquet, C., Basei, M., Hollanda, M., Rocher, S., Alasino, P., Moreno, G., 2019. Mid-crustal deformation in a continental margin orogen: structural evolution and timing of the Famatinian Orogeny, NW Argentina. J. Geol. Soc (in press).

Larrovere, M.A., Suzaño, N., Ratschbacher, B.C., Sola, A., Alasino, P.H., Fuentes, M.G., Finch, M.A., 2017. Las fajas de cizalla Dúctil del basamento ígneo-metamórfico del NOA. Relatorio 20° Congreso Geológico Argentino 579–601.

Lee, C.T., Thurner, S., Paterson, S., Cao, W., 2015. The rise and fall of continental arcs: interplays between magmatism, uplift, weathering, and climate. Earth Planet Sci. Lett. 425, 105–119.

Leng, W., Gurnis, M., 2015. Subduction initiation at relic arcs. Geophys. Res. Lett. 42, 7014–7021.

Lieu, W.K., Stern, R.J., 2019. The robustness of Sr/Y and La/Yb as proxies for crust thickness in modern arcs. Geosphere 15, 621–641.

López, J.P., Toselli, A.J., 1993. La faja milonítica TIPA: faldeo oriental del Sistema de

Famatina, Argentina. Acta 11° Congreso Geológico Argentino 3, 39–42.
Mángano, M., Astini, R., Buatois, L., Dávila, F., 2003. The ordovician system in the Famatina belt, depositional and tectonic evolution. Ser. Correlación Geol. 16, 295–312.
Mángano, M., Buatois, L., 1996. Shallow marine event sedimentation in a volcanic arc-related setting: the Ordovician Suri Formation, Famatina Range, northwest Argentina. Sediment. Geol. 105, 63–90.
Mángano, M., Buatois, L., 1997. Slope–apron deposition in an Ordovician arc–related setting, the Vuelta de Las Tolas member (Suri Formation), Famatina basin, northwest Argentina. Sediment. Geol. 109, 155–180.
Mannheim, R., 1993. Genese der Vulkanite und Subvulkanite des altpaläozoischen Famatina-Systems, NW-Argentinien, und Seine geodynamische Entwicklung. Munchner Geol. Hefte 7, 1–155.
Martino, R.D., 2003. Las fajas de deformación dúctil de las Sierras Pampeanas de Córdoba, una reseña general. Rev. Asoc. Geol. Argent. 58, 549–571.
Martino, R.D., Astini, R.A., 1998. La faja milonítica del Cordón de La Cumbre, Sistema del Famatina, La Rioja, Argentina. Actas 10° Congreso Latinoamericano de Geología 2, 37.
McCulloch, M.T., Gamble, J.A., 1991. Geochemical and geodynamic constraints on subduction zone magmatism. Earth Planet Sci. Lett. 102, 358–374.
Morosini, A., Enriquez, E., Ortiz Suárez, A., Ramos, G., Carugno Duran, A., Ulacco, J., 2014. Hipótesis de extrusión vinculada a la inversión metamórfica del Complejo Metamórfico Pringles, sierra de San Luis. Actas 19° Congreso Geológico Argentino S21–S38.
Morosini, A., Ortiz Suárez, A., Otamendi, J., Pagano, D., Ramos, G., 2017. La Escalerilla pluton, San Luis Argentina: the orogenic and post-orogenic magmatic evolution of the famatinian cycle at Sierras de San Luis. J. S. Am. Earth Sci. 73, 100–118.
Mulcahy, S., Roeske, S., McClelland, W., Ellis, J., Jourdan, F., Renne, P., Vujovich, G.I., 2014. Multiple migmatite events and cooling from granulite facies metamorphism within the Famatina arc margin of northwest Argentina. Tectonics 33, 1–25.
Müntener, O., Ulmer, P., 2018. Arc crust formation and differentiation constrained by experimental petrology. Am. J. Sci. 318, 64–89.
Nandedkar, R., Ulmer, P., Müntener, O., 2014. Fractional crystallization of primitive, hydrous arc magmas: an experimental study at 0.7 GPa. Contrib. Mineral. Petrol. 167, 1015.
Oliveros, V., Vásquez, P., Creixell, C., Lucassen, F., Ducea, M.N., Ciocca, I., González, J., Espinoza, M., Salazar, E., Coloma, F., Kasemann, S., 2020. Lithospheric evolution of the pre-and early andean convergent margin, Chile. Gondwana Res. 80, 202–227.
Ortiz Suárez, A., Casquet, M.C., 2005. Inversión metamórfica en el orógeno famatiniano de la Sierra de San Luis, Argentina. Geogaceta 38, 231–234.
Otamendi, J., Ducea, M., Bergantz, G., 2012. Geological, petrological and geochemical evidence for progressive construction of an arc crustal section, Sierra de Valle Fértil, Famatinian Arc, Argentina. J. Petrol. 53, 761–800.
Otamendi, J., Ducea, M., Tibaldi, A., Bergantz, G., de la Rosa, J., Vujovich, G., 2009. Generation of tonalitic and dioritic magmas by coupled partial melting of gabbroic and metasedimentary rocks within the deep crust of the Famatinian magmatic arc, Argentina. J. Petrol. 50, 841–873.
Otamendi, J., Pinotti, L., Basei, M., Tibaldi, A., 2010. Evaluation of petrogenetic models for intermediate and silicic plutonic rocks from the Sierra de Valle Fértil–La Huerta, Argentina, Petrologic constraints on the origin of igneous rocks in the Ordovician Famatinian–Puna paleoarc. J. S. Am. Earth Sci. 30, 29–45.
Otamendi, J., Tibaldi, A., Vujovich, G., Viñao, G., 2008. Metamorphic evolution of migmatites from the deep Famatinian arc crust exposed in sierras Valle Fértil–La Huerta, san juan, Argentina. J. S. Am. Earth Sci. 25, 313–335.
Pankhurst, R., Rapela, C., 1998. Introduction. Geol. Soc., Lond., Spec. Publ. 142, 1–9.
Pankhurst, R.J., Rapela, C.W., Saavedra, J., Baldo, E., Dahlquist, J., Pascua, I., Fanning, C.M., 1998. The Famatinian magmatic arc in the central Sierras Pampeanas: an Early to Mid-Ordovician continental arc on the Gondwana margin. Geol. Soc. Lond., Spec. Publ. 142, 343–368.
Pankhurst, R.J., Rapela, C.W., Fanning, C.M., 2000. Age and origin of coeval TTG, I- and S-type granites in the Famatinian belt of NW Argentina. Trans. R. Soc. Edinb. Earth Sci. 91, 151–168.
Paterson, S.R., Ducea, M.N., 2015. Arc magmatic tempos: gathering the evidence. Elements 11, 91–98.
Perón Orrillo, J., Ortiz Suárez, A., Rivarola, D., Otamendi, J., Morosini, A., Leisen, M., Romero, R., Barra, F., 2019. Depositional age and provenance in the San Luis Formation, Sierras Pampeanas, Argentina, evidence from detrital zircon studies. J. S. Am. Earth Sci. 94, 102228.
Petterson, M.G., 2018. The plutonic crust of Kohistan and volcanic crust of Kohistan–Ladakh, north Pakistan/India: lessons learned for deep and shallow arc processes. Geol. Soc. Lond., Spec. Publ. 483, SP483–S484.
Plank, T., Langmuir, C.H., 1988. An evaluation of the global variations in the major element chemistry of arc basalts. Earth Planet Sci. Lett. 90, 349–370.
Putirka, K.D., 2017. Down the crater, where magmas are stored and why they erupt. Elements 13, 11–16.
Ramos, V., 2018. The Famatinian orogen along the proto-margin of Western Gondwana, Evidence for a nearly continuous Ordovician magmatic arc between Venezuela and Argentina. In: The Evolution of the Chilean–Argentinean Andes. Springer, pp. 133–161.
Ramos, V., Cristallini, E., Pérez, D., 2002. The Pampean flat–slab of the central Andes. J. S. Am. Earth Sci. 15, 59–78.
Rapela, C.W., Coira, B., Toselli, A., Saavedra, J., 1992. The Lower Paleozoic magmatism of southwestern Gondwana and the evolution of Famatinian orogen. Int. Geol. Rev. 34, 1081–1142.
Rapela, C., Pankhurst, R., Casquet, C., Fanning, C., Baldo, E., González-Casado, J., Galindo, C., Dahlquist, J., 2007. The Río de la Plata craton and the assembly of SW Gondwana. Earth Sci. Rev. 83, 49–82.
Rapela, C., Pankhurst, R., Casquet, C., Dahlquist, J., Fanning, C., Baldo, E., Galindo, C., Ramacciotti, C., Verdecchia, S., Murra, J., Basei, M., 2018. A review of the Famatinian Ordovician magmatism in southern South America, evidence of lithosphere reworking and continental subduction in the early proto–Andean margin of Gondwana. Earth Sci. Rev. 187, 259–285.
Ratschbacher, B.C., Paterson, S.R., Fischer, T.P., 2019. Spatial and depth-dependent variations in magma volume addition and addition rates to continental arcs: application to global CO_2 fluxes since 750 Ma. G-cubed 20, 2997–3018.
Ringwood, A.E., 1974. The petrological evolution of island arc systems, Twenty–seventh William Smith Lecture. J. Geol. Soc. 130, 183–204.
Rossi, J.N., Toselli, A.J., Báez, M.A., 2005. Evolución termobárica del ortogneis peraluminoso del noroeste de la sierra de Velasco, La Rioja. Rev. Asoc. Geol. Argent. 60, 278–289.
Saal, A., 1993. El basamento cristalino de la sierra de Paganzo, provincial de La Rioja, Argentina. Thesis (unpublished). Universidad de Córdoba, Córdoba, pp. 1–206.
Saavedra, J., Toselli, A., Rossi, J., Pellitero, E., Durand, F., 1998. The early palaeozoic magmatic record of the Famatina system: a review. Geol. Soc., Lond., Spec. Publ. 142, 283–295.
Saleeby, J.B., 1990. Progress in tectonic and petrogenetic studies in an exposed cross–-section of young (~ 100 Ma) continental crust, southern Sierra Nevada, California. In: Exposed Cross–Sections of the Continental Crust. Springer, pp. 137–158.
Schmidt, M.W., Jagoutz, O., 2017. The global systematics of primitive arc melts. G-cubed 18, 2817–2854.
Schmidt, M.W., Poli, S., 1998. Experimentally based water budgets for dehydrating slabs and consequences for arc magma generation. Earth Planet Sci. Lett. 163, 361–379.
Schwartz, J., Gromet, L.P., Miro, R., 2008. Timing and duration of the calc-alkaline arc of the pampean orogeny: implications for the late Neoproterozoic to Cambrian evolution of western Gondwana. J. Geol. 116, 39–61.
Semenov, I., Weinberg, R.F., Taylor, R.J., Jourdan, F., 2019. Prolonged movement on a > 10-km-wide thrust during early Paleozoic orogens in the Gondwana margin of NW Argentina. Tectonics 38, 3210–3236.
Simpson, C., Law, R.D., Gromet, L.P., Miró, R., Nothrup, C.J., 2003. Paleozoic deformation in the sierras de Córdoba and sierra de las Minas, eastern Sierras Pampeanas, Argentina. J. S. Am. Earth Sci. 15, 749–764.
Sims, J., Ireland, T., Camacho, A., Lyons, P., Pieters, P., Skirrow, R., Stuart-Smith, P., Miró, R., 1998. U-Pb, Th-Pb and Ar-Ar geochronology from the southern Sierras Pampeanas, Argentina: implications for the Paleozoic tectonic evolution of the western Gondwana margin. Geol. Soc. Lond., Spec. Publ. 142, 256–281.
Snyder, D., Ramos, V., Allmendinger, R., 1990. Thick-skinned deformation observed on deep seismic reflection profiles in western Argentina. Tectonics 9, 773–788.
Stern, R.J., 2002. Subduction zones. Rev. Geophys. 40 3–1.
Stern, R.J., Bloomer, S.H., 1992. Subduction zone infancy: examples from the Eocene Izu-Bonin-Mariana and Jurassic California arcs. Geol. Soc. Am. Bull. 104, 1621–1636.
Tatsumi, Y., Hamilton, D., Nesbitt, R., 1986. Chemical characteristics of fluid phase released from a subducted lithosphere and origin of arc magmas: evidence from high-pressure experiments and natural rocks. J. Volcanol. Geoth. Res. 29, 293–309.
Tibaldi, A., Barzola, M., Cristofolini, E., Otamendi, J., Demichelis, A., Leisen, M., Romero, R., Barra, F., Camilletti, G., Armas, P., 2019. Syn-deformational anatexis along the Santa Rosa river section, Argentina: feedback relations between deformation, metamorphism and melt extraction. J. Struct. Geol. 124, 151–167.
Tibaldi, A., Otamendi, J., Gromet, L., Demichelis, A., 2008. Suya Taco and Sol de Mayo mafic complexes from eastern Sierras Pampeanas, Argentina: evidence for the emplacement of primitive OIB-like magmas into deep crustal levels at a late stage of the Pampean orogeny. J. S. Am. Earth Sci. 26, 172–187.
Tibaldi, A., Otamendi, J., Cristofolini, E., Baliani, I., Walker Jr., B., Bergantz, G., 2013. Reconstruction of the Early Ordovician Famatinian arc through thermobarometry in lower and middle crustal exposures, Sierra de Valle Fértil, Argentina. Tectonophysics 589, 151–166.
Tollan, P., Hermann, J., 2019. Arc magmas oxidized by water dissociation and hydrogen incorporation in orthopyroxene. Nat. Geosci. 12, 667–671.
Toselli, A.J., Durand, F., Rossi, J.N., Saavedra, J., 1996. Esquema de evolución geotectónica y magmática Eopaleozoica del Sistema de Famatina y sectores de Sierras Pampeanas. Actas 13° Congreso Geológico Argentino Actas 5, 443–462.
Toselli, A.J., Saavedra, J., Pellitero, E., Rossi, J.N., Aceñolaza, F.G., Medina, M., 1990. Geoquímica y petrogenesis del volcanismo ordovícico de la Formación Las Planchadas, Sistema de Famatina. Rev. Asoc. Geol. Argent. 45, 313–322.
Toth, J., Gurnis, M., 1998. Dynamics of subduction initiation at preexisting fault zones. J. Geophys. Res.: Solid Earth 103, 18053–18067.
Turner, J.C., 1960. Estratigrafía del tramo medio de la Sierra de Famatina y adyacencias. La Rioja. Boletín Academia Nacional de Ciencias 42, 77–126.
Vaccari, N., Benedetto, J., Waisfeld, B., Sánchez, T., 1993. La fauna de Neseuretus en la Formación Suri (oeste de Argentina), edad y relaciones paleobiogeográficas. Rev. Esp. Palaontol. 8, 185–190.
Vaccari, N., Waisfeld, B., 1993. Nuevos trilobites de la Formación Suri (Ordovícico Temprano) en la región de Chaschuil, provincia de Catamarca. Implicancias bioestratigráficas. Ameghiniana 31, 73–86.
Verdecchia, S., Baldo, E., Benedetto, J., Borghi, P., 2007. The first shelly faunas from metamorphic rocks of the Sierras Pampeanas (La Cébila Formation, Sierra de Ambato, Argentina), age and paleogeographic implications. Ameghiniana 44, 493–498.
Verdecchia, S., Collo, G., Baldo, E., 2011. Polyphase white mica growth in low–grade metapelites from La Cébila Metamorphic Complex (Famatinian Belt, Argentina), evidence from microstructural and XRD investigations. Andean Geol. 38, 2.
von Gosen, W., Prozzi, C., 1998. Structural evolution of the sierra de San Luis (eastern sierras Pampeanas, Argentina): implications for the proto-andean margin of Gondwana. Geol. Soc. Lond., Spec. Publ. 142, 235–258.

von Gosen, W., Prozzi, C., 2005. Deformation of an early paleozoic magmatic arc related to terrane collision: the sierra de San Luis (eastern sierras Pampeanas, Argentina). Neues Jahrbuch Geol. Palaontol. Abhand. 238, 107–160.
Walker Jr., B., Bergantz, G., Otamendi, J., Ducea, M., Cristofolini, E., 2015. A MASH zone revealed, the mafic complex of the Sierra Valle Fértil. J. Petrol. 56, 1863–1896.
Whitmeyer, S., Simpson, C., 2003. High strain-rate deformation fabrics characterize a kilometers-thick Paleozoic fault zone in the Eastern Sierras Pampeanas, central Argentina. J. Struct. Geol. 25, 909–922.
Whitmeyer, S., Simpson, C., 2004. Regional deformation of the sierra de San Luis, Argentina: 1056 implications for the paleozoic development of western Gondwana. Tectonics 23, 1–16.
Wolfram, L., Weinberg, R., Nebel, O., Hamza, K., Hasalová, P., Míková, J., Becchio, R., 2019. A 60–Myr record of continental back–arc differentiation through cyclic melting. Nat. Geosci. 12 (3), 215.
Yin, A., 2006. Cenozoic tectonic evolution of the Himalayan orogen as constrained by along-strike variation of structural geometry, exhumation history, and foreland sedimentation. Earth Sci. Rev. 76, 1–131.